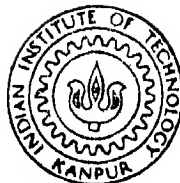


# KINETICS OF PRECIPITATE COARSENING IN A HIGH STRENGTH LOW ALLOY STEEL CONTAINING Ti AND V

*By*

**MAHESH KUMAR AGARWAL**

ME  
1993  
M  
AGA  
KIN



**DEPARTMENT OF METALLURGICAL ENGINEERING**  
**INDIAN INSTITUTE OF TECHNOLOGY KANPUR**  
**APRIL, 1993**

KINETICS OF PRECIPITATE COARSENING IN A HIGH STRENGTH LOW ALLOY  
STEEL CONTAINING Ti AND V

*A Thesis Submitted  
in Partial Fulfilment of the Requirements  
for the Degree of*  
MASTER OF TECHNOLOGY

by

MAHESH KUMAR AGARWAL

*to the*

DEPARTMENT OF METALLURGICAL ENGINEERING  
INDIAN INSTITUTE OF TECHNOLOGY KANPUR

April , 1993

ME-1993-M-AGA-KIN

LIBRARY  
21 JUL 2003 MLT  
No A116134  
A116134

7h  
669.1  
1

26/4/93

## CERTIFICATE

This is to certify that the present work, entitled Kinetics of Precipitate Coarsening in a High Strength Low Alloy Steel Containing Ti and V, by Mahesh Kumar Agarwal has been carried out under my supervision and it has not been submitted elsewhere for a degree



April, 1993

Dr Shant P Gupta  
Professor  
Department of Metallurgical Engineering  
Indian Institute of Technology  
Kanpur

## ACKNOWLEDGEMENT

I wish to express my deep sense of indebtedness and gratitude to Dr S P Gupta, Professor, Department of Metallurgical Engineering, IIT Kanpur, who proposed, guided and helped this work to completion through his uncountable suggestions and encouragement

I am grateful to Mr K S Rao, Rajesh, Narshimha, Govind and many other friends for their immense help and nice company without their timely assistance the work would not have completed in time My sincere thanks to Mr R P Singh, Mr Barthwal, Mr M N Mangole, Mr K P Mukherjee for their technical assistance

In the last I would like to thank Mr Yash Pal for an excellent job of typing at the shortest notice of time

April 1993  
Kanpur

Mahesh Kumar Agarwal

---

*DEDICATED  
TO MY  
PARENTS*

## CONTENT

	Page No
ABSTRACT	i
LIST OF FIGURES	ii
LIST OF TABLES	iv
LIST OF SYMBOLS	v
CHAPTER 1 INTRODUCTION	1
1 1 Volume Diffusion Controlled Coarsening	7
1 2 particle Size Distribution	11
1 3 Effect of Volume Fraction of the Precipitate	13
1 4 Estimation of $Q$ and $D_0$	17
CHAPTER 2 EXPERIMENTAL PROCEDURE	18
2 1 Material	18
2 2 Replica Preparation	20
2 3 Transmission Electron Microscopic Studies	20
2 4 Particle Size Measurement	21
2 5 Actual Magnification Calibration	21
2 6 Particle Size Distribution	21
CHAPTER 3 RESULT AND DISCUSSION	22
3 1 Morphology	22
3 2 Coarsening Behaviour of Precipitate	22
3 3 Particle Size Distribution	25
3 4 Kinetics of Coarsening	43
CHAPTER 4 CONCLUSIONS	50
REFERENCES	51
APPENDIX	53

## ABSTRACT

The coarsening behaviour of carbonitride precipitate has been examined in a high strength low alloy steel (HSLA) containing 0.105 wt % Ti and 0.089 wt % V as carbonitride forming elements in the temperature range 733–770°C. The steel was aged for periods ranging from 1 h to 343 h at 733°C, 752°C and 770°C temperatures. Transmission Electron Microscopy was carried out on carbon extraction replica. Particle size distributions (PSDs) were determined for various aging times at the three aging temperatures. Although  $\bar{r}^3 = kt$  rate law was observed during coarsening, none of the presently available coarsening theories showed complete agreement with the experimental particle size distribution. A normal distribution rather than a log-normal distribution was observed. The value of volume diffusivity,  $D_v$ , is observed to be comparable with the corresponding published value.



## LIST OF FIGURES

Figure No	Captions	Page No
Fig 1 1	Free energy-composition diagram illustrating the driving force for coarsening	2
Fig 1 2	A polydisperse assembly of particles	2
Fig 1 3	Concentration - distance profile on a particle which is growing	5
Fig 1 4	Theoretical particle size distribution as predicted by the LSW[5], BW[8], BWEM[9], and VG[10] theories. The steady-state distribution are presented for the BW and BWEM theories at precipitate volume fraction of 60% and for the VG theory at 50 Vol % [Ref 15]	5
Fig 1 5	A polydisperse assembly of particles showing the mean free path	15
Fig 1 6	The effect of the volume fraction on the parameter $\eta$	15
Fig 2 1	The extraction replica technique (a) Polished surface (b) Etched to expose second phase, (c) Carbon coated, and (d) re-etched and replica floated off [Ref 11]	19
Fig 3 1	TEM Micrograph of extraction replica, specimen aged for 64 hours at 770°C	23
Fig 3 2	Electron diffraction pattern derived from a isolated precipitate particle	23
Fig 3 3	TEM Micrograph showing vanadium Titanium Carbonitride as cube geometry, specimen aged 216 hours at 752°C	24
Fig 3 4	In TEM Micrograph Cube Shaped particles appeared as slightly rounded	24
Fig 3 5	Transmission Electron Micrograph specimen aged at 770°C (a) aged for 8 minutes (b) aged for 216 hours	26
Fig 3 6	Transmission electron micrograph specimen aged at 752°C (a) aged for 8 hours (b) aged for specimen 64 hours	27

Fig 3 7	Transmission Electron Micrograph specimen aged at 733°C (a) aged for 8 minutes (b) aged for 1 hour	28
Fig 3 8	Particle size distribution, specimen aged at 770°C (a) aged for 8 minutes (b) aged for 1 hour (c) aged for 8 hours (d) aged for 27 hours (e) aged for 64 hours (f) aged for 216 hours	30 31 32
Fig 3 9	Particle size distribution specimen aged at 752°C (a) Aged for 8 minutes (b) Aged for 1 hour (c) Aged for 8 hours (d) Aged for 64 hours (e) Aged for 137 hours (f) Aged for 216 hours (g) Aged for 343 hours	33 34 35 36
Fig 3 10	Particle size distribution specimen aged at 733°C (a) Aged for 8 minutes (b) Aged for 1 hour (c) Aged for 64 hours (d) Aged for 216 hours (e) Aged for 343 hours	37 38
Fig 3 11	Theoretical PSD modified to accommodate the volume fraction of the precipitate [Ref 5]	40
Fig 3 12	Theoretical PSD modified to incorporate the encounters between particles [Ref 7]	41
Fig 3 13	$\bar{a}$ versus $t^{1/3}$ plot for the coarsening of vanadium Titanium Carbonitride (VTiCN) in HSLA Steel	45

## LIST OF TABLES

Table No	Title	Page No
Table 2 1	Composition of HSLA Steel in Wt/	19
Table 3 1	Average particle size with respect to time and temperature	44
Table 3 2	Value of the Constant ( $\bar{a}_0$ ) and slope $(K)^{1/3}$	47
Table 3 3	Value of $K$ , $^{\infty}X_B^{\alpha}$ , $D_v$ experimental and calculated	48

## LIST OF SYMBOLS

Symbol	Meaning
$r_{X_B}^{\alpha}$	Solute concentration in the matrix at the precipitation - matrix interface of a particle of $r$ (Mole fraction)
$\omega_{X_B}^{\alpha}$	Solute concentration in the matrix at the precipitation - matrix interface of a large particle (Mole fraction)
$V_m^{\beta}$	Molar volume of the phase ( $m^3/\text{mole}$ )
$\nu_i$	Interracial free energy of the $i$ th face
$h$	Time in hour
$T$	Temperature ( $^{\circ}K$ )
$R$	Gas constant ( $8.31434 \text{ J K}^{-1} \text{ mole}^{-1}$ )
$J_1$	The flux to the particle from the matrix
$J_2$	The flux arising out of the growth of particles
$\bar{r}$	Average particle radius at time $t$
$\bar{r}_0$	Average particle at the onset of coarsening
$D_v$	Coefficient of diffusion of the solute in the matrix
$D_0$	Rate constant
$Q$	Activation energy
$\frac{dR}{dt}$	Growth rate
$\rho$	The ratio of the edge length to the average edge length ( $a/\bar{a}$ )
$g(\rho)$	Normalized distribution function
$K$	Slope of line plotting inbetween $(\bar{a})^3$ vs $t$ ( $m^3/\text{sec}$ )

# CHAPTER 1

## INTRODUCTION

The mechanical properties of HSLA steel are strongly dependent upon the size and distribution of the carbide precipitate. Since the carbide particle can coarsen during the initial heat treatment and during subsequent service, it is important to be able to predict the kinetics of coarsening. The ideas of precipitate coarsening was first formulated by Ostwald [1] as early as in 1900. The precipitate coarsening describes the change in average particle size with increasing time. It results from higher solubility of small particles, which may tend to dissolve in the matrix and cause the growth of larger particles. The driving force is provided by the reduction in total interfacial energy of the system when the average particle size increases with time. This can be best illustrated with the help of the free energy-composition diagram, Figure 1.1. Let us consider a large spherical particle of radius  $r$  being surrounded by a number of smaller particles whose average radius is  $\bar{r}$ , Figure 1.2. A common tangent construction between  $G_m^\alpha$  and  $G_m^\beta$  phases of the free energy - composition diagram established equilibrium between the two phases. Such construction indicates that large particles have lower solubility of the solute in the matrix in which they are contained. It is clear from the figure 1.1 that when large particles grow at the expense of smaller particles, there is a reduction in the interfacial energy per unit volume of the material. The energy thus released acts as driving force for

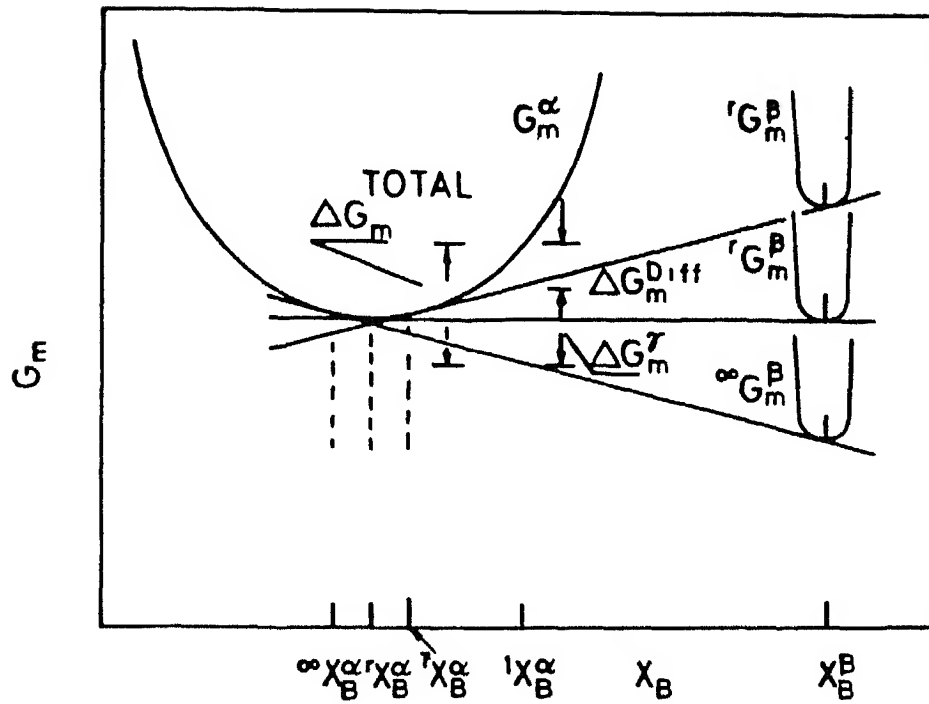


Fig 1 1 Free energy-composition diagram illustrating the driving force for coarsening

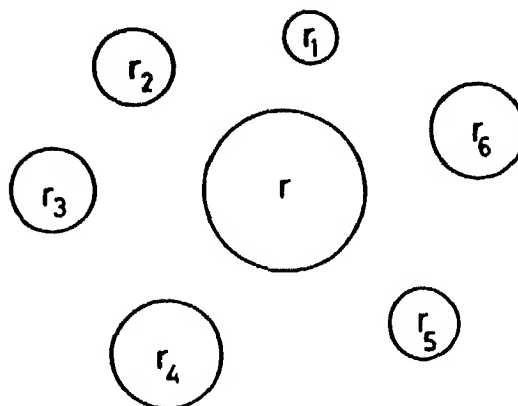


Fig 1 2 A polydisperse assembly of particles

the coarsening reaction

Because of the importance of the precipitate stability in commercial alloys the coarsening of precipitates has been studied experimentally by numerous investigators. Detailed theoretical analysis of the kinetics of coarsening was carried out by Lifschitz and Slyozov [2] and independently by Wagner [3] in what has become to be known as the LSW theory of coarsening. The principal finding of the LSW theory is that the average particle size increases with the cube root of the time of coarsening.

The solubility of a particle in the matrix as a function of its radius is best illustrated by the Gibbs - Thomson equation, written as

$$\ln \left[ \frac{r_{X_B}^{\alpha/\beta}}{\omega_{X_B}^{\alpha/\beta}} \right] = \frac{V_m^\beta \gamma}{RT} \frac{dA}{dV} \quad (1.1)$$

where

$r_{X_B}^{\alpha/\beta}$  = Solubility of a particle of radius  $r$ ,

$\omega_{X_B}^{\alpha/\beta}$  = Solubility of a particle of infinite radius,

$V_m^\beta$  = Molar Volume of the precipitate,

$\gamma$  = Interfacial free energy,

$\frac{dA}{dV}$  = Rate of change of surface area of the precipitate

with volume and  $R$  &  $T$  have their usual meaning

For spherical particles of radius of  $r$

$$A = 4\pi r^2, \quad V = \frac{4}{3} \pi r^3$$

So the term  $dA/dV$  in equation (1.1) equals  $2/r$  which upon substitution yields

$$\ln \left[ \frac{r_{X_B}^{\alpha/\beta}}{\omega_{X_B}^{\alpha/\beta}} \right] = \frac{2V_m^\beta \gamma}{RT r} \quad (1.2)$$

Assuming typical values of the terms on the right hand side of equation (1 2)

$$\begin{aligned}\gamma &= 100 \text{ mJ/m}^2 \\ R &\approx 8314 \text{ J/mole}^\circ\text{K} \\ T &= 1000^\circ\text{K} \\ V_m^\beta &= 10 \times 10^{-6} \text{ m}^3/\text{mole} \\ r &= 10^{-7} \text{ to } 10^{-8} \text{ m}\end{aligned}$$

Then

$$\frac{2V_m^\beta \gamma}{RT r} = \frac{2 \times 100 \times 10 \times 10^{-6} \times 10^{-3}}{8314 \times 1000 \times 10^{-7}} = 2.4 \times 10^{-3}$$

Since the term on the right hand side has a small value, equation (1 2) is written as

$$\left[ r_{X_B}^{\alpha/\beta} - \omega_{X_B}^{\alpha/\beta} \right] = \frac{2V_m^\beta \gamma \omega_{X_B}^{\alpha/\beta}}{RT r} \quad (1.3)$$

If an isolated particle of the precipitate phase is rich in solute then the concentration distance profile in the early stages of its growth is as shown in Figure 1.3. However, nucleation of precipitate particles in the vicinity of an isolated particles and their continued growth make the diffusion field overlap. The particles stop growing thereafter. New region cannot nucleate solute-rich  $\beta$  phase because the neighbouring matrix is depleted of solute. The smaller particles dissolve during coarsening and the solute thus released moves down the concentration gradient (built gradually from smaller to larger particles) to attach themselves to larger particles. The process of coarsening therefore is one where some particles are continuously dissolving, some are continuously growing and some remain quasi-stationary at any given small time interval. During this interval some



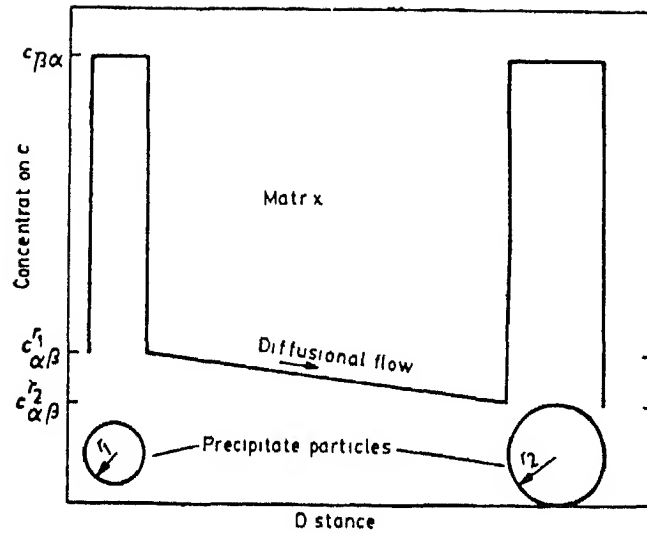


Fig 1 3 Concentration - distance profile on a particle which is growing

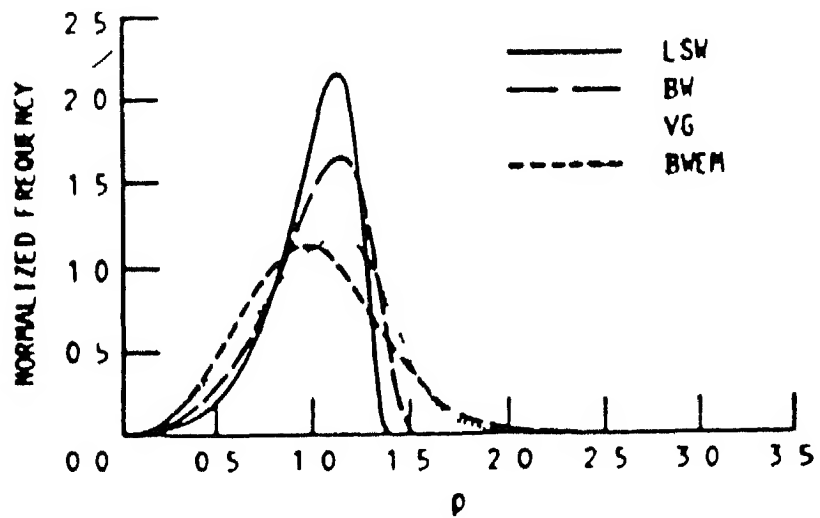


Fig 1 4 Theoretical particle size distribution as predicted by the LSW[5], BW[8], BWEM[9], and VG[10] theories. The steady-state distribution are presented for the BW and BWEM theories at precipitate volume fraction of 60% and for the VG theory at 50 Vol / [Ref 15]

particles must have dissolved completely and disappeared. The particles which remain quasi-stationary, i.e., which is neither growing nor dissolving at any given small time interval is termed as the critical size particle of radius  $r^*$ . It is understood that particles that remained quasi-stationary in a given interval may not be so in subsequent intervals. This is so because with the coarsening of particles, the average particle size increases and the critical particle size also increases with it. The net results being that the number of particles remaining after any time interval decreases with time and the average particle size increases with time.

There are a number of coarsening mechanisms. These are

- 1 Volume diffusion controlled
- 2 Ledge mechanism
- 3 Grain boundary diffusion - controlled
- 4 Diffusion through dislocations
- 5 Interface controlled

When the rate controlling mechanism is the diffusion of solute through the regular lattice sites, the coarsening mechanism is said to be volume diffusion controlled (VDC). In order to establish a functional relationship between the particle size and the time of coarsening, it is essential to make some simplified assumption. These are

- 1 The concentration gradient is considered to be time independent. This will allow us to use Fick's first law to adequately describe the concentration gradient under steady state conditions.

- 2 The solute diffusion coefficient,  $D$  is independent of concentration of the solute. This condition will again be fulfilled because dilute solutions are generally used in precipitation studies.
- 3 The interfacial energy of the  $\alpha/\beta$  interface  $\gamma_{\alpha\beta}$ , is independent of the radius of curvature. This is quite critical below particle size of  $100\text{\AA}$  or so. Since the size of the particle at the termination of growth is of the order of  $100\text{\AA}$ , the interfacial energy will not be seriously affected during coarsening. Thus a constant value of  $\gamma_{\alpha\beta}$  will be assumed for the entire coarsening process.
- 4 For spherical particles, the effective diffusion distance is considered to be proportional to the radius of curvature of the particle. The value of the proportionality constant,  $\alpha$ , which in reality is a complicated non-analytical function of several variables is assumed to remain constant during the entire coarsening process.

### 1.1 Volume Diffusion Controlled Coarsening

For spherical particles of radius  $r$ , the flux  $J_1$  to the particle from the matrix is given by the Fick's first Law as

$$J_1 = -D \cdot 4\pi r^2 \frac{\Delta x_{\beta}^{\alpha}}{\Delta x} \quad (1.4)$$

Where  $D$  = rate of diffusion of solute through the lattice

$4\pi r^2$  = surface area of the sphere

$\Delta x$  = effective diffusion distance

From the Gibbs-Thomson's effect, equation (1.3), the solute concentration difference  $\Delta x_{\beta}$  is given as

$$\Delta x_B = \left[ r x_B^{\alpha/\beta} - \bar{r} x_B^{\alpha/\beta} \right] = \omega_{x_B}^{\alpha/\beta} \frac{2\nu V_m^\beta}{RT} \left[ \frac{1}{r} - \frac{1}{\bar{r}} \right]$$

and

$\Delta x$  effective =  $\alpha r$

which upon substitution in equation (1.4) yields

$$J_1 = -D 4\pi r^2 \omega_{x_B}^{\alpha/\beta} \frac{2\nu V_m^\beta}{\alpha RT r^2} \left[ 1 - \frac{1}{r} \right] \quad (1.5)$$

The flux  $J_1$  can be equated to the flux  $J_2$  arising out of the growth of spherical shaped particle from the matrix which gives

$$J_2 = \left[ x_B^\beta - x_B^\alpha \right] \frac{dV}{dt} = \left[ x_B^\beta - \bar{x}_B^\alpha \right] 4\pi r^2 \frac{dr}{dt} = J_1 \quad (1.6)$$

Where

$V$  = Volume of the sphere and

$$\left[ x_B^\beta - \bar{x}_B^\alpha \right] = \text{Solute concentration difference across the } \alpha/\beta \text{ boundary}$$

Upon equating the flux equation for  $J_1$  and  $J_2$  and rearranging terms, we get

$$\frac{dr}{dt} = - \frac{2D V_m^\beta \nu \omega_{x_B}^{\alpha/\beta}}{\alpha RT (x_B^\beta - x_B^\alpha) r^2} \left[ 1 - \frac{r}{\bar{r}} \right] \quad (1.7)$$

On rearranging the terms of equation (1.7) and integrating on both sides we get

$$\int_{\frac{r_0}{1-\frac{r_0}{\bar{r}}}}^{\bar{r}} \frac{r^2 dr}{r^2 (1-\frac{r}{\bar{r}})} = - \int_0^t \frac{2D \nu V_m^\beta \omega_{x_B}^{\alpha/\beta}}{\alpha RT (x_B^\beta - x_B^\alpha)} dt \quad (1.8)$$

Treating as constant and applying results of the LSW theory, equation (1.8) becomes

$$\frac{\bar{r}^3}{3} - \frac{r_0^3}{3} = \frac{8}{9} D \nu \frac{V_m^\beta \omega_{x_B}^{\alpha/\beta}}{\alpha RT (x_B^\beta - x_B^\alpha)} t \quad (1.9)$$

Where  $\bar{r}$  is the average particle radius after time  $t$ ,  $\bar{r}_0$  is the average particle radius at the onset of coarsening  $D_v$  is the diffusion coefficient of the solute in the matrix and other terms have already been defined

D Ramkrishna and S P Gupta [4] derived the equation for platelets shape particle by volume diffusion controlled coarsening They consider square platelets of edge length  $a$  and thickness  $h$  If the interfacial energies of the broad face and the edge with the  $\alpha$  matrix are  $\nu_F$  and  $\nu_e$  respectively, application of the Gibbs Theomson equation yields

$$\ln \left( \frac{X_B^\alpha}{\omega_{X_B}^\alpha} \right) = \frac{V_m^\beta}{RT} \frac{4h\nu_e + 4a\nu_F}{2ah} \quad (1.10)$$

Where  $X_B^\alpha$  and  $\omega_{X_B}^\alpha$  are the solubilities of particle of any size and a very large size respectively and  $V_m^\beta$  is the molar volume of the  $\beta$  phase

From the Gibbs-Wulff theorem, The following can be written

$$\frac{2\nu_F}{h/2} = \frac{2\nu_e}{a/2} = W \quad (1.11)$$

Where  $W$  is the Wulff constant, which on substitution in equation (1.11) gives the solubility difference between particles of edge length  $a$  and mean value  $\bar{a}$  as

$$\Delta X_B^\alpha = \frac{4\nu_e V_m^\beta \omega_{X_B}^\alpha}{RT} \left[ \frac{1}{\bar{a}} - \frac{1}{a} \right] \quad (1.12)$$

The flux  $J_1$  to the particle from the Fick's first Law is

$$J_1 = -D_v (2a^2 + 4ah) \frac{4\nu_e V_m^\beta \omega_{X_B}^\alpha}{RT\alpha(a/2)a} \left[ 1 - \frac{a}{\bar{a}} \right] \quad (1.13)$$

Where  $\alpha a/2$  is the diffusion distance,  $D_v$  is the volume diffusion coefficient and  $2a^2 + 4ah$  is the area through which diffusion takes place The flux  $J_1$  is equated to the flux  $J_2$

arising out of the growth of particles as follows

$$J_2 = \left[ x_B^\beta - x_B^\alpha \right] \frac{d}{dt} \left\{ 4 \left( \frac{a}{2} \right)^2 h \right\} = -D_v (2a^2 + 4ah) \frac{4\nu_e \sqrt{\beta} \omega x_B^\alpha}{RT\alpha a^2/2} \left[ 1 - \frac{a}{\bar{a}} \right] \quad (1.14)$$

Letting  $h = \alpha/\beta$ , differentiating and rearranging yields

$$\int_{a_0/2}^{a/2} \frac{(a/2)^2 d(a/2)}{(1 - \frac{a}{\bar{a}})} = - \int_0^t \frac{2}{3} D_v (\beta + 2) \frac{\nu_e \sqrt{\beta} \omega x_B^\alpha}{RT\alpha} dt \quad (1.15)$$

The parameter  $\beta$  is related to the specific interfacial energies of the two interfaces and can be calculated. Treating  $\alpha$  as a constant and applying results of the Lifshitz-Slyozov-Wagner theory gives

$$\left( \frac{\bar{a}}{2} \right)^3 - \left( \frac{\bar{a}_0}{2} \right)^3 = \frac{8}{27} (\beta + 2) D_v \frac{\nu_e \sqrt{\beta} \omega x_B^\alpha}{\alpha RT (x_B^\beta - x_B^\alpha)} t \quad (1.16)$$

Except for the numerical factor  $8/27 (\beta + 2)$ , equation (1.16) is identical in form with the kinetics equation of Wagner (3). Substitution for  $\beta = 1$  ( $h=a$ ) enables the kinetics equation for the coarsening of cube-shaped precipitates to be obtained

$$\left( \frac{\bar{a}}{2} \right)^3 - \left( \frac{\bar{a}_0}{2} \right)^3 = \frac{8}{9} \frac{D_v \nu_e \sqrt{\beta} \omega x_B^\alpha}{\alpha RT (x_B^\beta - x_B^\alpha)} t \quad (1.17)$$

$$(\bar{a})^3 - (\bar{a}_0)^3 = \frac{64}{9} \frac{D_v \nu_e \sqrt{\beta} \omega x_B^\alpha}{\alpha RT (x_B^\beta - x_B^\alpha)} t \quad (1.18)$$

Equation (1.18) can be written in an approximate form

$$\bar{a} = (Kt)^{1/3} \quad (1.19)$$

where

$$K(\text{Rate constant}) = \frac{64}{9} \frac{D_v \nu \sqrt[3]{m} X_B^\alpha}{\alpha RT (X_B^\beta - X_B^\alpha)}$$

## 1.2 Partical Size Distribution

Given sufficient time of coarsening of the precipitate after initial growth, particle which are larger than the average will grow and those smaller than the average size will gradually shrink and disappear. Thus a particle size distribution function,  $f(r, t)$  can be defined that corresponds to the number of particles of a given radius  $r$  at time  $t$ . The total number of particle  $n_p$  in the system at any instant is given by

$$n_p = \int_0^{\infty} f(r, t) dr$$

initially,  $n_p$  is constant and equals the number of particles at the end of the growth process of the precipitate. However, as some particles grow, some dissolve and others remain stationary during coarsening, the particle size distribution broadens. The distribution of particle sizes evolves towards a quasi-steady state distribution,  $f(r, t)$ , which is independent of the initial distribution  $f(r, 0)$ . The distribution function is written as

$$f(r, t) = f(t) \rho^2 h(\rho) \quad (1.20)$$

Where  $f(t)$  is function of time only

$$\rho = \frac{r}{\bar{r}}$$

and  $h(\rho)$  as solved by Wagner for a Gaussian distribution is

$$h(\rho) = \left[ \frac{3}{3+\rho} \right]^{7/3} \left[ \frac{3/2}{\frac{3}{2} - \rho} \right]^{11/3} \exp \left[ - \frac{\rho}{3/2 - \rho} \right] \quad (1.21)$$

From which

$$h(\rho) = 0 \quad \text{for } \rho = \rho_m = 3/2$$

$\rho_m$  being one cut-off radius ratio also known as the maximum relative radius of the particle. Taking  $f(r,t) \propto \rho^2 h(\rho)$ , it is clear that,

$$\text{for } \rho = 0, \quad f(r,t) = 0$$

$$\text{and for } \rho = 3/2 \quad f(r,t) = 0$$

This implies a sharp cut-off in the distribution, such that no precipitate particles exist with radius more than 1.5 times the mean radius of the particles. The distribution has a maximum value at  $\rho = 1.135$ .

Following Wagner's approach [3], the integration can be carried out for

$$\rho = \frac{r}{r^*} = \frac{r}{\bar{r}} = \frac{3}{2} \text{ yielding}$$

$$\int_{\frac{3}{2}\bar{r}_0}^{\frac{3}{2}\bar{r}} \frac{\bar{r}^2 d\bar{r}}{1 - \frac{3}{2}} = \frac{2D v_{\alpha\beta} V_m^{\beta\infty} X_B^\alpha}{\alpha RT (X_B^\beta - X_B^\alpha)} t \quad (1.22)$$

or

$$(\bar{r})^3 - (\bar{r}_0)^3 = \frac{8}{9} \frac{D v_{\alpha\beta} V_m^{\beta\infty} X_B^\alpha}{\alpha RT (X_B^\beta - X_B^\alpha)} t \quad (1.23)$$

Although the cube rate law has been exhibited by a number of alloys. The experimental particle size distribution (PSDs) do not coincide with the prediction of the LSW [5] theory. This discrepancy is mainly attributed to the fact that the LSW theory is strictly applicable when the precipitate volume fraction is small and approaches zero. Obviously this zero volume fraction



approximation is not valid for many material systems. As a result, considerable effort has gone into modifying the basic theory. For example, Lifshitz-Slyozov Encounter Modified (LSEM) theory. It has been shown by Davies et al. [7] which considers encounter between precipitate particles, the Brailsford-Wynblatt (BW) [8], the Brailsford-Wynblatt Encounter Modified (BWEM) [9], and the Voorhees-Glicksman (VG) [10] theories.

The theoretical PSD's predicted by the LSW [5], the BW [8], BWEM [9], and the VG [10], theories are shown in Figure 1.4. The latter three theories have attempted to incorporate the influence of finite precipitate volume fraction. Figure 1.4 shows the steady state distribution which are predicted by the BW and BWEM theories for alloys with 60 vol / precipitate and by the VG theory for alloys with 50 Vol/ precipitate. In the present study, the experimental PSD's were determined as a function of time and temperature.

### 1.3 Effect of Volume Fraction of the Precipitate

The theory of particle coarsening by Lifshitz and Slyozov and Wagner (LSW), is applicable only when the volume fraction of the precipitate is very small, under the condition, the mean distance between particles is large compared to the dimension of the particle. Since the kinetics of coarsening is controlled by the diffusion of solute from a particle which is dissolving to a particle which is growing, it is expected that the mean distance between particles which is controlled in turn by the volume fraction,  $V_f$  of the precipitate will influence the rate of growth. As  $V_f$  increases, the mean separation between particles decreases and the distance that solute atoms have to diffuse on an average

to become a part of the growing precipitate become shorter. A detailed analysis of the problem has been treated by Ardell [5] by considering a distribution of particle sizes surrounding an  $i$ th particle of radius  $r_i$ , as shown in Figure 1.5. If the mean free path between the  $i$ th particle and its neighbour is  $\bar{X}$  then, for a polydispersed assembly of particles, the distance  $r$  at which the solute concentration in the matrix approaches the solute concentration of the particle - matrix interface of average size particle is given by

$$r = r_i + \frac{\bar{X}}{2} \quad (1.24)$$

In order to introduce the effect of the volume fraction on the rate of coarsening, a relation between  $r$  and  $V_f$  must be obtained. This relation is difficult to obtain for a polydisperse assembly. However, when the particles are considered to be all of the same radius  $r^*$ , the center to center distance,  $d$ , between a particle and its nearest neighbour is

$$d = r^* \left[ 2 + \frac{8V_f}{3^{3/2}\gamma V_f} \Gamma(V_f) \right] \quad (1.25)$$

where the gamma function,

$$\Gamma(V_f) = \int_{8V_f}^{\infty} y^{-2/3} e^{-y} dy$$

Now, from figure 1.5,  $\bar{X} = d - 2r^*$

$$= \frac{8V_f}{3^{3/2}\gamma V_f} \Gamma(V_f) r^* \quad (1.26)$$

$$\text{and } r = r_i + \frac{r^*}{2} \frac{8V_f}{3^{3/2}\gamma V_f} \Gamma(V_f) \quad (1.27)$$

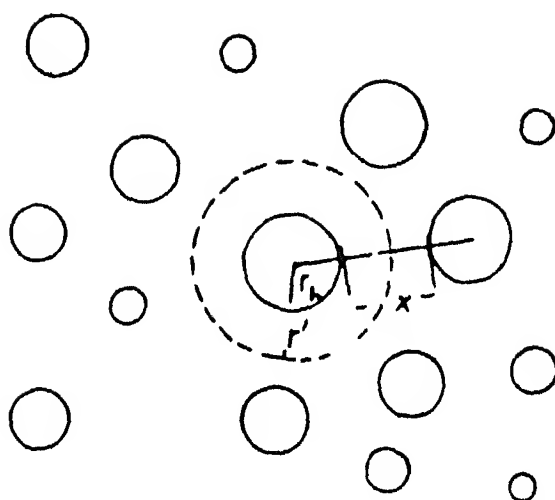


Fig 1 5 A polydisperse assembly of particles showing the mean free path

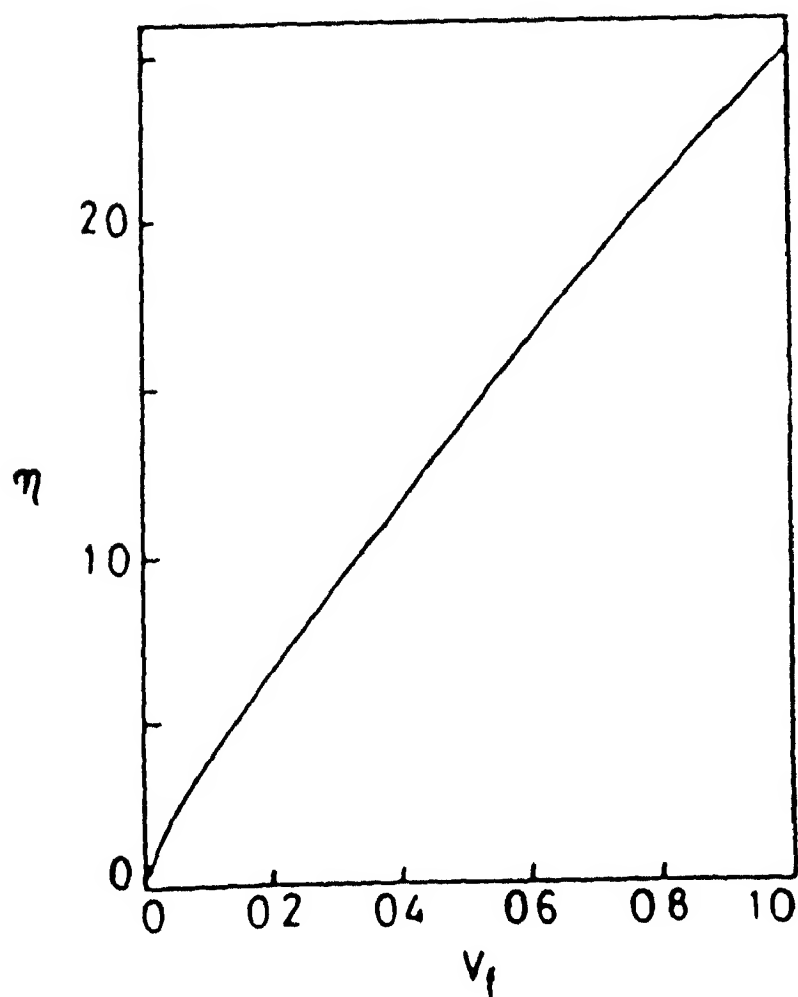


Fig 1 6 The effect of the volume fraction on the parameter  $\eta$

$$\text{or } \frac{r}{r^*} = 1 + \frac{1}{\eta P} \quad (1.28)$$

$$\text{where } \eta = \frac{2 \gamma v_f}{e^{BV} f(v_f)} \quad \text{and } P = \frac{r}{r^*}$$

The effect of volume fraction on the parameter  $\eta$  is shown in Figure 1.6

Rate equation which is as follows

$$\frac{dr^3}{dt} = \frac{6D \nu_{\alpha\beta} V_m^{1/3} \omega_{XB}^\alpha}{RT (X_B^\beta - X_B^\alpha)} (1 + \eta P) (\rho - 1)$$

or,

$$r^{*3} - r_o^{*3} = \frac{6D \nu_{\alpha\beta} V_m^{1/3} \omega_{XB}^\alpha}{RT (X_B^\beta - X_B^\alpha) \psi} t \quad (1.29)$$

Where  $r_o^*$  is the critical radius of the particle in the initial distribution

$r^*$  is critical size which is neither growing nor dissolving

$$\psi = \frac{6D \nu_{\alpha\beta} V_m^{1/3} \omega_{XB}^\alpha}{RT (X_B^\beta - X_B^\alpha)} \frac{dt}{dr^{*3}}$$

$$\bar{\rho} = \frac{\bar{r}}{r^*} \text{ which upon substitution in equation (1.14)}$$

$$(\bar{r})^3 - (\bar{r}_o)^3 = \frac{6D \nu_{\alpha\beta} V_m^{1/3} \omega_{XB}^\alpha}{RT (X_B^\beta - X_B^\alpha) \psi} (\bar{\rho})^3 t \quad (1.30)$$

The value of  $\bar{\rho}$  has been calculated by Ardell [5] and it is found to have weak dependence on the volume fraction of the precipitate. In the range that most studies of coarsening are carried out,  $\bar{\rho}$  increases from approximately 0.94 to 1.0 as the volume fraction decreases from 0.1 to zero.

#### 1.4 Estimation of $Q$ and $D_0$

Equation (1.19) is of the form  $y = K^{1/3}x$  where  $K^{1/3}$  indicates the slope of the line. From a plot of  $\bar{x}$  vs  $t^{1/3}$  at different temperatures and  $D_v$  can be calculated. The Arrhenius equation is

$$D_v = D_0 \exp^{-Q/RT} \quad (1.31)$$

where  $D_v$  is the diffusion rate,  $D_0$  is the rate constant

$Q$  is the activation energy and

$R$  &  $T$  have their usual meaning

Upon substitution of the value of  $D$  in equation (1.19) we get

$$K = \frac{64}{9} \frac{D_0 v \sqrt[3]{m} \omega_X^\alpha}{\alpha R T (X_B^\beta - X_B^\alpha)} \exp^{-Q/RT} \quad (1.32)$$

This can be written as

$$KT = \frac{64}{9} \frac{D_0 v \sqrt[3]{m} \omega_X^\alpha}{\alpha R (X_B^\beta - X_B^\alpha)} \exp^{-Q/RT} \quad (1.33)$$

$$\text{or } KT = A \exp^{-Q/RT}$$

$$\text{or } \ln KT = \ln A - \frac{Q}{RT}$$

where

$$A = \frac{64}{9} \frac{D_0 v \sqrt[3]{m} \omega_X^\alpha}{\alpha R (X_B^\beta - X_B^\alpha)}$$

We can determine the diffusion parameters  $D_0$  and  $Q$  from the intercept and slope of the straight line respectively from the Arrhenius plot. On comparing the theoretical and experimental values of  $D_0$  and  $Q$  one can predict the mechanism that is operating for the growth of precipitates.

## CHAPTER 2

### EXPERIMENTAL PROCEDURE

#### 2.1 Material

The present investigation was carried out to study the kinetics of precipitate coarsening in a HSLA Steel containing Ti and V. The HSLA steel containing 0.1% Vanadium and 0.08% Titanium was obtained in the hot forged condition from Climax Molybdenum Corporation U.S.A. Table 2.1 shows the composition of this steel in the as-received condition. It contains small amount of nitrogen which makes Vanadium nitride and Titanium nitride precipitation possible during isothermal aging. The elements Si and Al are in very minor quantity and thus will have negligible influence. The sole function of these two elements will be in contributing to solid solution strengthening. The addition of Mn retards the rate of growth of ferrite from Austenite.

The steel had been hot forged to obtain rounds 18 mm in diameter and then cold rolled with a number of intermediate annealing treatments to obtain section 3 mm thick. Small square specimen size  $6 \times 6 \text{ mm}^2$  were solution treated for 8 minutes. Isothermal transformation was carried out at temperatures  $733^\circ\text{C}$ ,  $752^\circ\text{C}$  and  $770^\circ\text{C}$  in sealed quartz tube under vacuum for 1 h to 15 days.

The experimental procedure and the techniques used for the study of kinetics of precipitate coarsening are as described in the following sections.

Table 2 1  
Composition of HSLA Steel (in Wt %)

Element	C	N	Si	Al	Mn	V	Ti
Amount	0.1	0.016	0.09	0.048	1.5	0.089	0.105

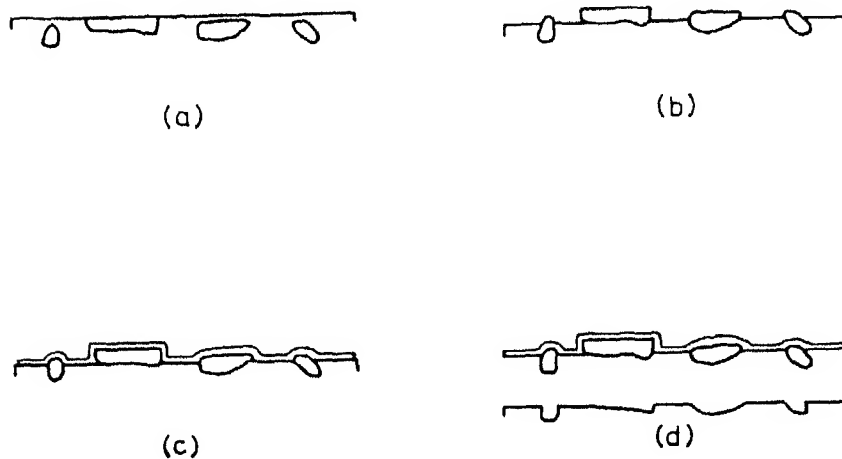


Fig 2 1 The extraction replica technique (a) Polished surface (b) Etched to expose second phase, (c) Carbon coated, and (d) re-etched and replica floated off [Ref 11]

## 2.2 Replica Preparation

In order to study the kinetics of precipitate coarsening of TiVCN the particle size and shapes were derived from carbon extraction replica technique. This technique is illustrated schematically in Figure 2.1. The two phase structure to be replicated was first etched sufficiently in a nital solution containing 3% nitric acid to expose the second phase. A thin layer of carbon coating was done in the usual way. Shadowing of carbon is to be avoided in order to ensure a strong continuous film and therefore, rotation of the specimen or diffuse deposition was done. Subsequently shadowing was used to give information about the three dimensional shape of the extracted particles. The specimen was next dipped in a nital solution containing 12% nitric acid so that the matrix was attacked while the second phase, which was to be extracted remained unchanged. The replica, containing particles of the second phase was collected on a copper grid. The most critical part of this procedure was the second etching to free the replica and particles from the base metal. It was necessary to score the carbon coating into squares before etching. This floating carbon film containing particles was collected on copper grid (dia = 3mm) for further study.

## 2.3 Transmission Electron Microscopic Studies

Carbon extraction replicas collected on copper grid were examined using the TEM (JEOL-2000FX). In order to confirm the shape and size of the precipitate sufficient number of photographs were taken and in order to confirm precipitate phase is indeed Vanadium Titanium carbonitride, selected area diffraction patterns were obtained from isolated large particle.

---



## 2.4 Particle Size Measurement

Edge length of the particle was measured manually with the help of a vernier caliper, having least count 0.002cm. From each sample measurements were made on approximately 500 particles.

## 2.5 Actual Magnification Calibration

The electron photomicrographs taken on 35 mm camera don't have magnification marker on them. In order to carry out the calibration the same features were recorded on both the 35 mm camera and plate camera at a number of magnifications. The plate camera had the magnification marker on it. The same precipitate particle size is measured in both the photograph and the actual magnification of 35 mm camera determined.

## 2.6 Particle Size Distribution

The particle size distribution data were obtained by feeding the raw data to a computer programmed to give mean particle size, size distribution and particle size ratio,  $a/\bar{a}$  for each specimen.

LIBRARY  
DEC. No A 116134

## CHAPTER 3

### RESULTS AND DISCUSSION

#### 3.1 Morphology

A photomicrograph of the precipitate during coarsening is shown in Figure 3.1, which is a transmission electron micrograph of extraction replica derived from a specimen aged for 64 hours at 770°C. It clearly shows the square cross section of the precipitate. In order to confirm it, the precipitate phase is indeed Vanadium-Titanium carbonitride (VTiCN), selected area diffraction pattern was obtained from isolated large particle as shown in Figure 3.2, as an illustration. It indexes as Face centered cubic (FCC) lattice. The cube geometry was maintained for the entire duration of coarsening as confirmed from the TEM micrograph of Figure 3.3 derived from a specimen aged for 216 hours at 752°C. During later stages of coarsening, there was a slight tendency for the edges of the cube to either get rounded or convert into small facets. With these modifications, the cube shaped particles appeared as slightly rounded as shown in Figure 3.4, derived from a specimen aged for 343 hours at 733°C. The square geometry was not eliminated, however.

#### 3.2 Coarsening Behaviour of Precipitate:

The coarsening behaviour of the VTiCN precipitate was examined as a function of temperature from 733°C to 770°C for the 0.081 wt% V, 0.0105 wt% Ti, 0.1 wt% C and 0.016 wt% N containing HSLA Steel. The TEM photomicrographs of Figure 3.5 depict the change in the microstructure which occurs during aging at 770°C.

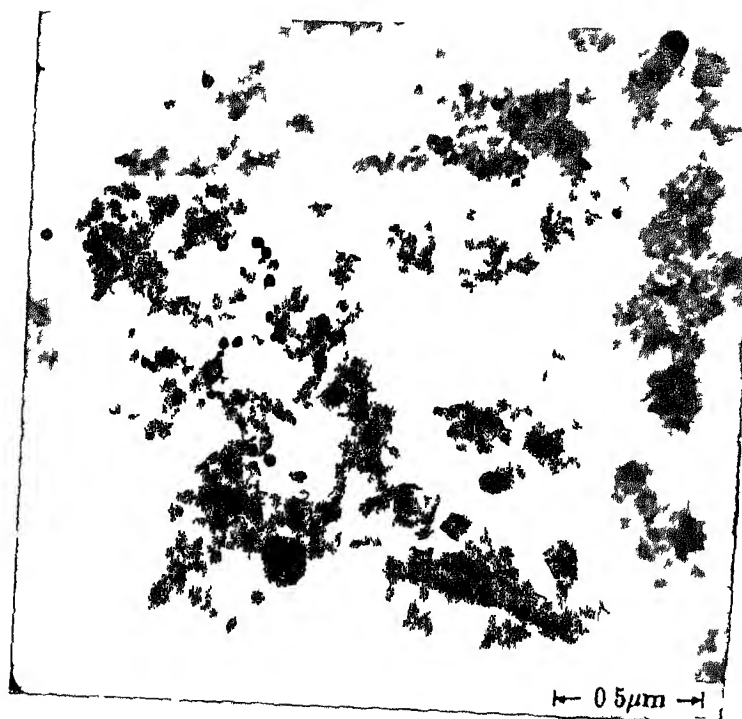


Fig 3 1 TEM Micrograph of extraction replica, specimen aged for 64 hours at 770°C

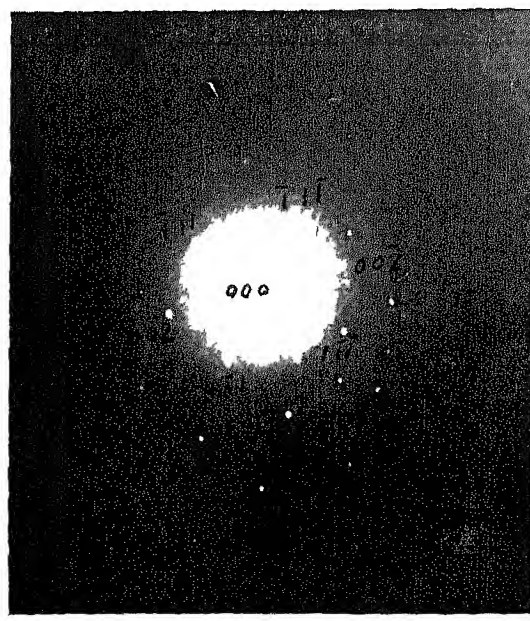


Fig 3 2 Electron diffraction pattern derived from a isolated precipitate particle

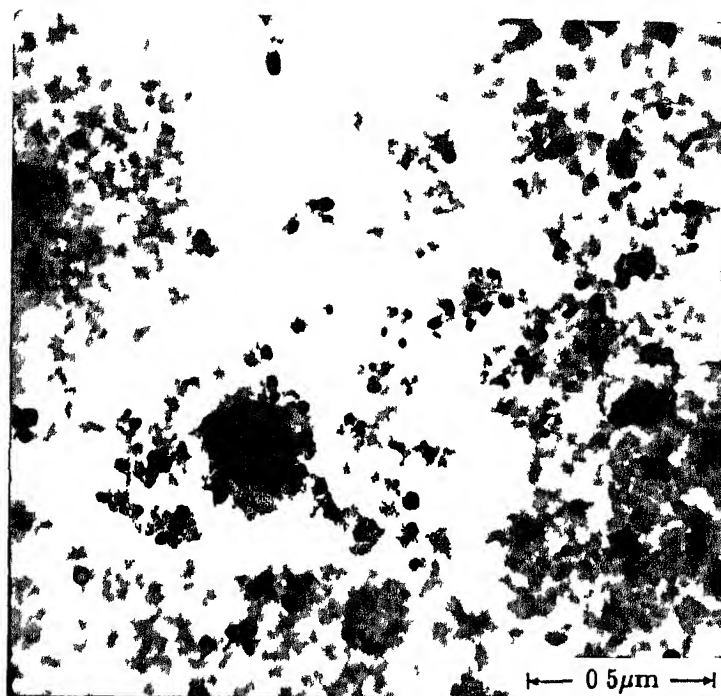


Fig 3 3 TEM Micrograph showing vanadium Titanium Carbonitride as cube geometry, specimen aged 216 hours at 752°C

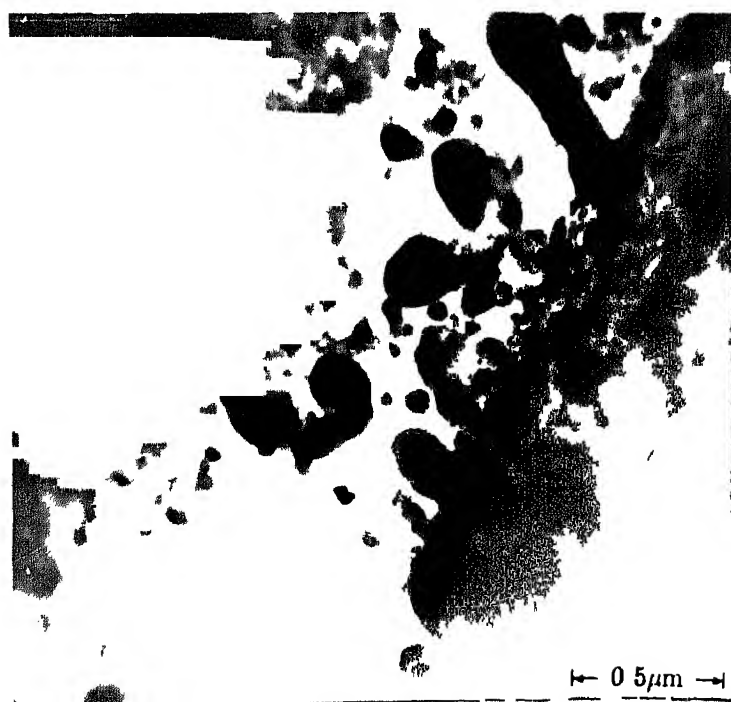


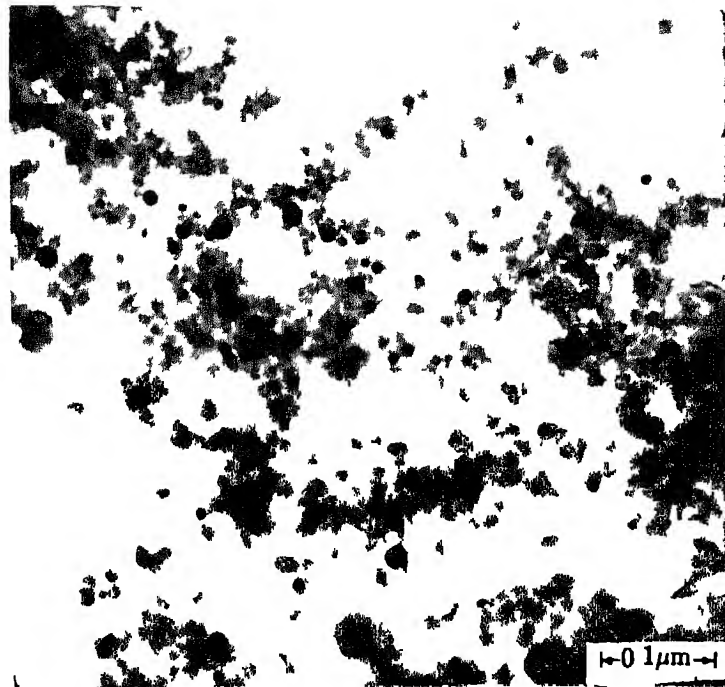
Fig 3 4 In TEM Micrograph Cube Shaped particles appeared as slightly rounded

for times of up to 216 hours. Figure 3.5(a) shows the initial micro structure after aging for 8 minutes. The precipitate particles in this condition were cubical in shape and had an average particle size,  $\bar{a} = 78.22$  angstrom. After aging for 1h, 8h, 27h, 64h and 216h the precipitate particles increase in size, but some were coalescing as well. Figure 3.5(b) derived from a specimen aged for 216 hours at  $770^{\circ}\text{C}$  shows the increased in average particle size.

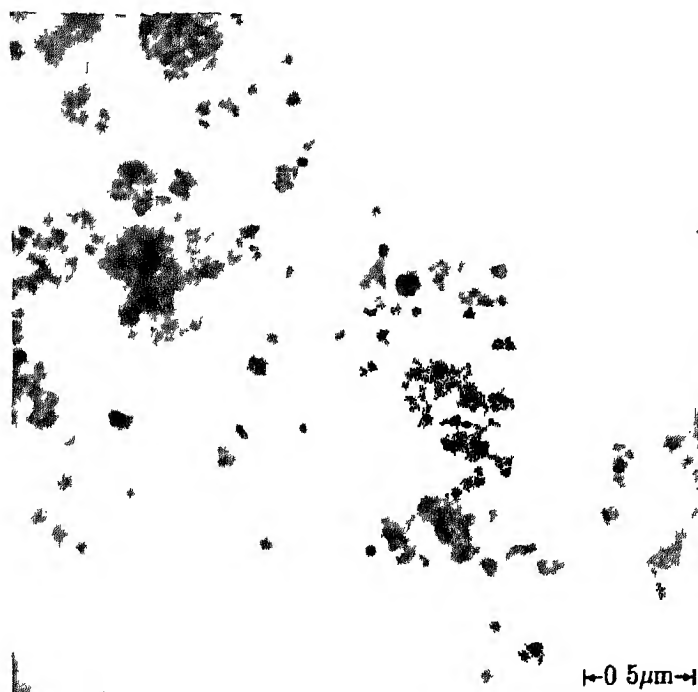
Similar results were obtained during coarsening at  $752^{\circ}\text{C}$  and  $733^{\circ}\text{C}$ . The precipitate particles were cubical in shape as shown in Figures 3.6(a) and 3.6(b) derived from specimens aged for 8 hours and 64 hours respectively at  $752^{\circ}\text{C}$ . Photomicrographs presented in Figures 3.7(a) and 3.7(b) show the precipitate particles derived from a specimen aged for 8 minutes and 64 hours respectively at  $733^{\circ}\text{C}$ .

### 3.3 Particle Size Distributions:

The initial particle size distribution after 8 minutes aging at  $770^{\circ}\text{C}$  is shown in Figure 3.8(a). The aging time was sufficient for complete transformation of austenite to ferrite at this temperature. The austenite to ferrite transformation initiates after an incubation period of few seconds and it is expected that the Vanadium Titanium Carbonitride particles that formed first must have coarsened to some extent in 8 minutes. This cannot be avoided, however, in this alloy system in which the second phase forms by interface controlled mechanism [12]. The coordinates of Figure 3.8(a) are  $g(\rho)$  and  $\rho$ . Where  $\rho(a/\bar{a})$  is the ratio of the edge length to the average edge length and  $g(\rho)$  is the normalized distribution function, i.e., the fraction of the particles that

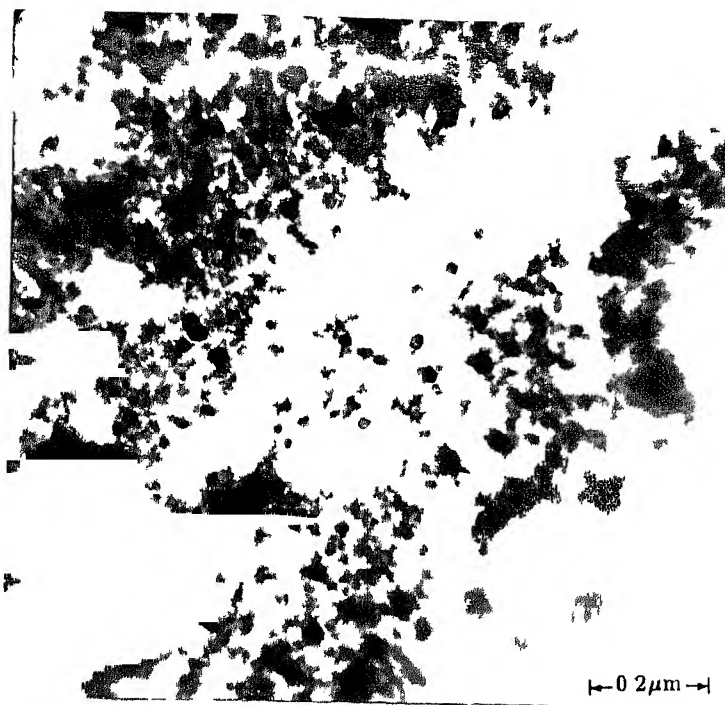


(a)

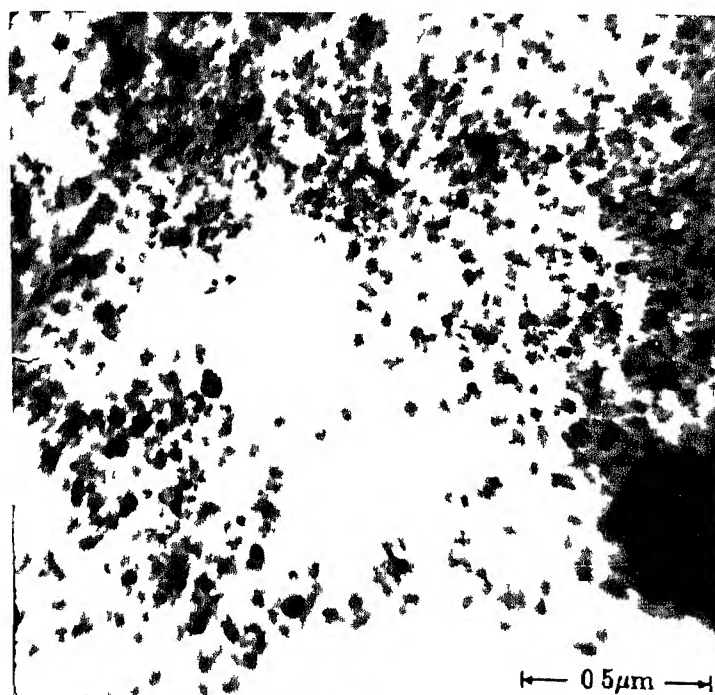


(b)

Fig 3 5 Transmission Electron Micrograph specimen aged at 770°C (a) aged for 8 minutes (b) aged for 216 hours

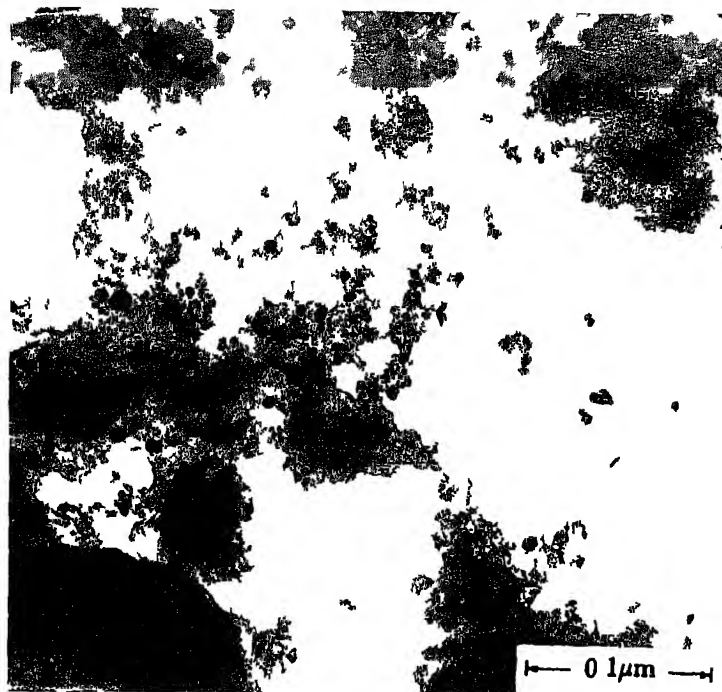


(a)

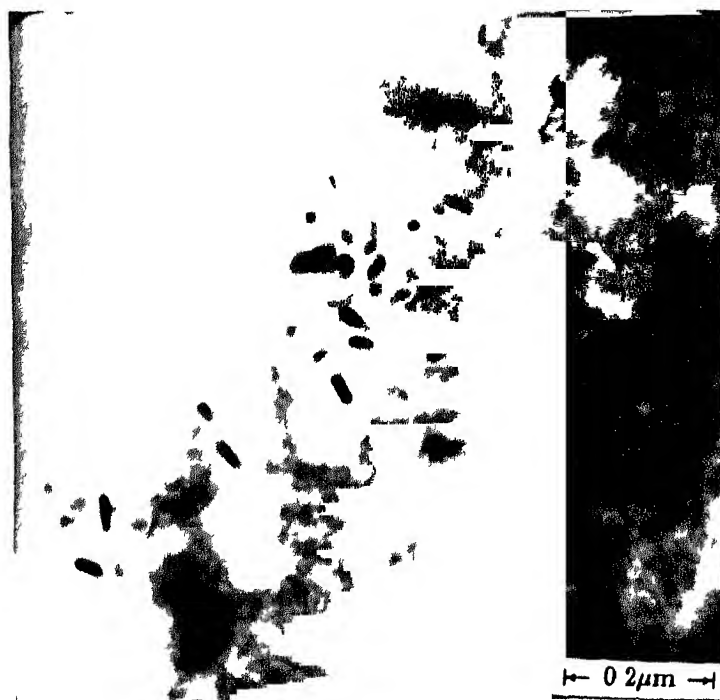


(b)

Fig 3 6 Transmission electron micrograph specimen aged at  $752^{\circ}\text{C}$   
 (a) aged for 8 hours (b) aged for specimen 64 hours



(a)



(b)

Fig 3 7 Transmission Electron Micrograph specimen aged at  $733^{\circ}\text{C}$   
 (a) aged for 8 minutes (b) aged for 64 hours



lie in an interval multiplied by the reciprocal of the interval itself

The particle size distributions after aging for 1h, 8h, 27h, 64h, 216h at 770°C are displayed in Figure 3 8(b), 3 8(c), 3 8(d), and 3 8(e) respectively. Values of  $\rho$  at which  $g(\rho)$  is maximum lie in the range of 1.2 to 2.0 and the cut off radius ratio,  $\rho_{\max}$ , lie in the range of 1.8 to 2.0. PSDs after coarsening for 8 minutes, 1h, 8h, 64h, 137h, 216h and 343h at 752°C are shown in Figure 3 9(a) - 3 9(g) respectively. PSDs for 8 minutes, 1 h, 64 h, 216 h and 343 h at 733°C are shown in Figure 3 10(a)-3 10(e) respectively. Values of  $\rho$  at which  $g(\rho)$  is maximum lie in the range of 1.0 to 1.8 and their cut off radius ratio  $\rho_{\max}$ , lie in the range of 1.8-2.0. Based on the particle size distribution displayed in Figure 3 8 to 3 10 at three different temperature, the following observations can be made

- (a) The particle size distributions for most aging condition were symmetrical about the mean value, indicating a normal distribution rather than a log normal distribution predicted by the Lifshitz, Slyozov and Wagner [2,3] theory. The coarsening of VC in a Vanadium bearing HSLA Steel is reported [4] to have similar PSDs.
- (b) The cut off diameter ratio,  $a/\bar{a}$  is reported to have value upto 1.9 instead of the cut off radius ratio  $\rho$  of 1.5 as predicted by LSW [2,3] theory for the volume diffusion controlled coarsening. A cut off radius ratio exceeding 1.5 has also been observed in a number of investigation, namely Ni-Co-Al [7], Al-Cu [13] and Fe-C-V [4].
- (c) The peak value of  $g(\rho)$  is observed to fall in the range

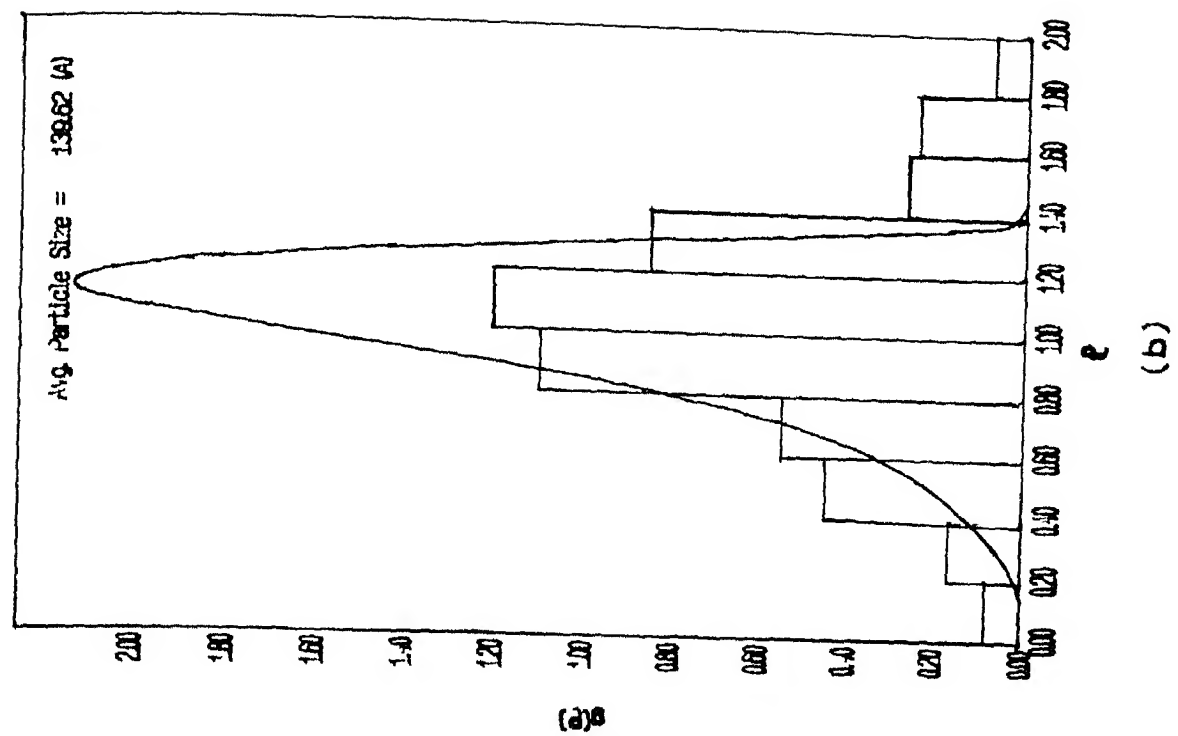
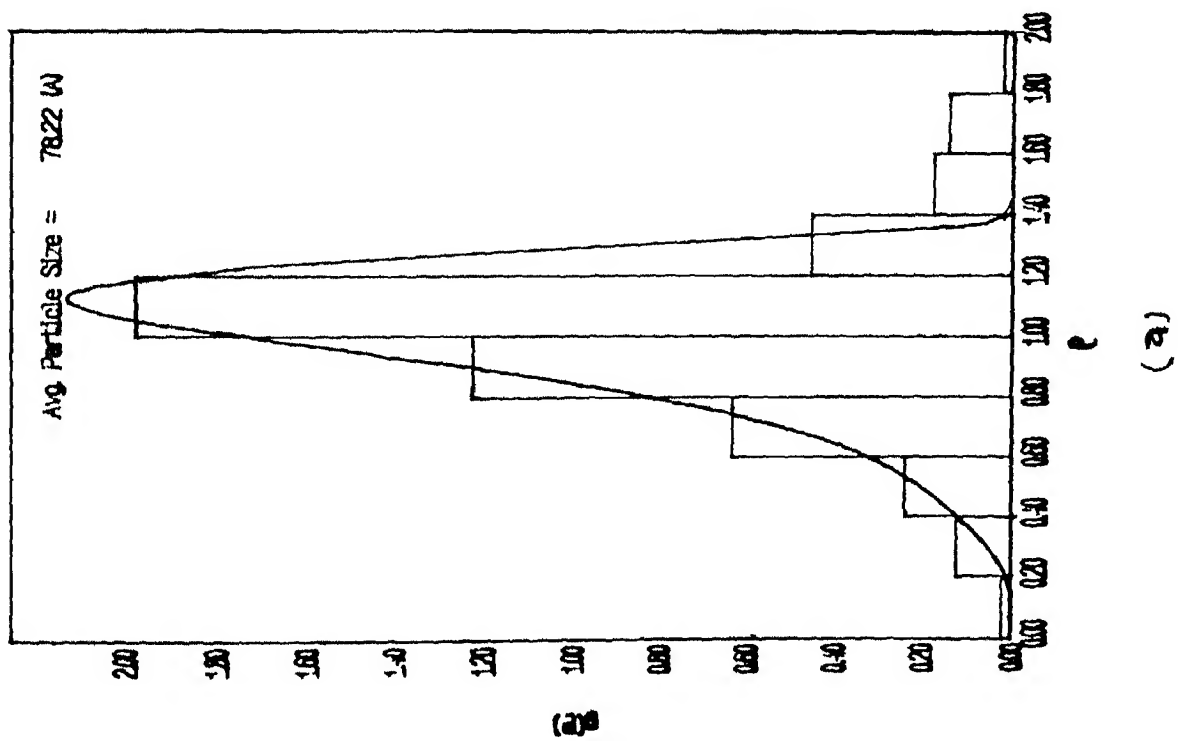


Fig 3.8 Particle size distribution, specimen aged at 770°C  
(a) aged for 8 minutes (b) aged for 1 hour

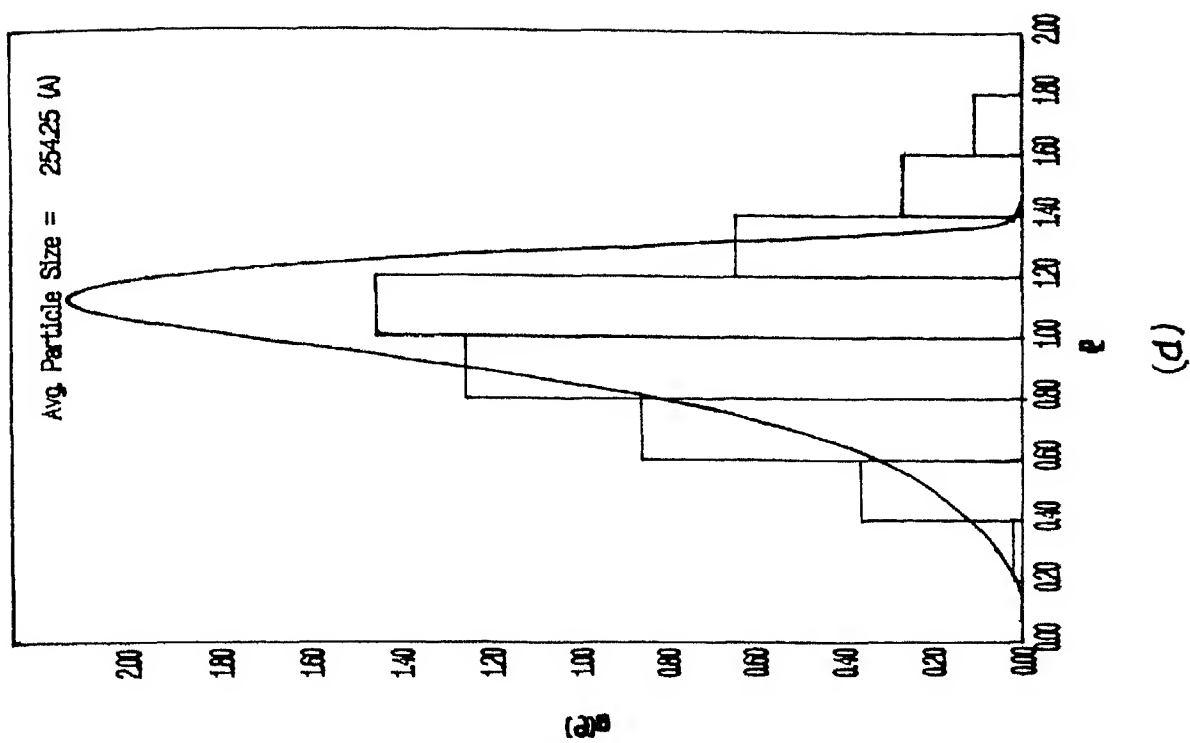
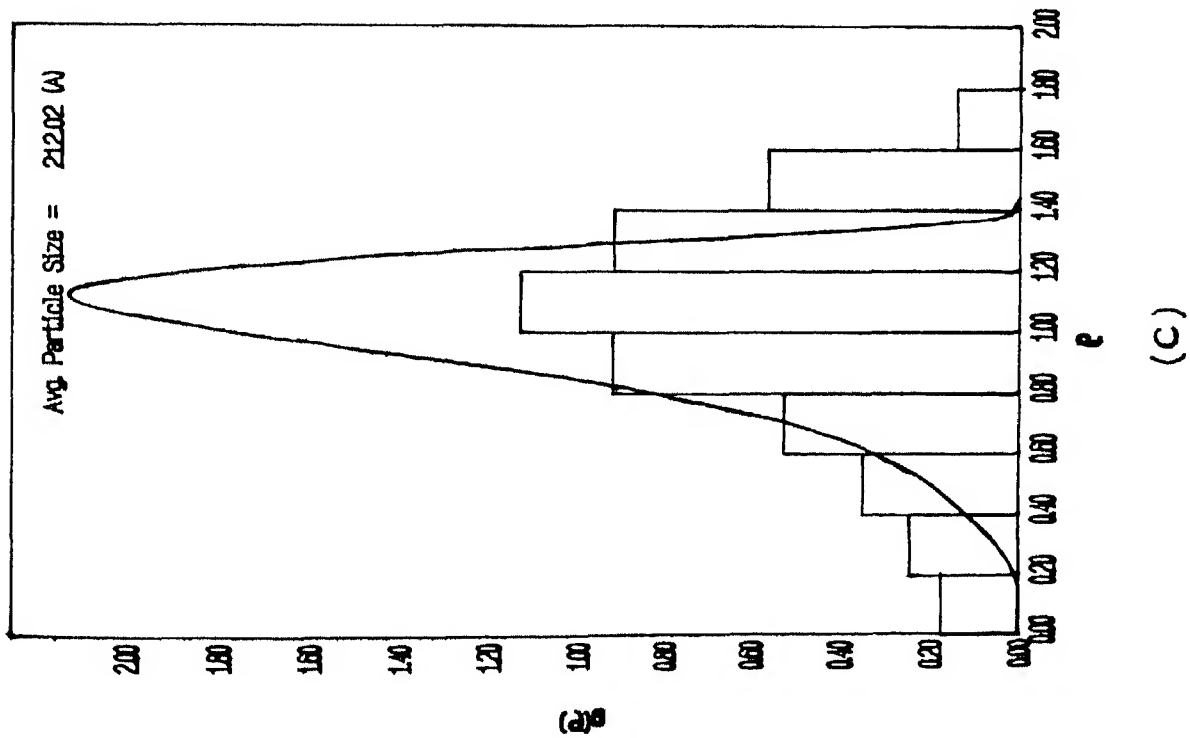
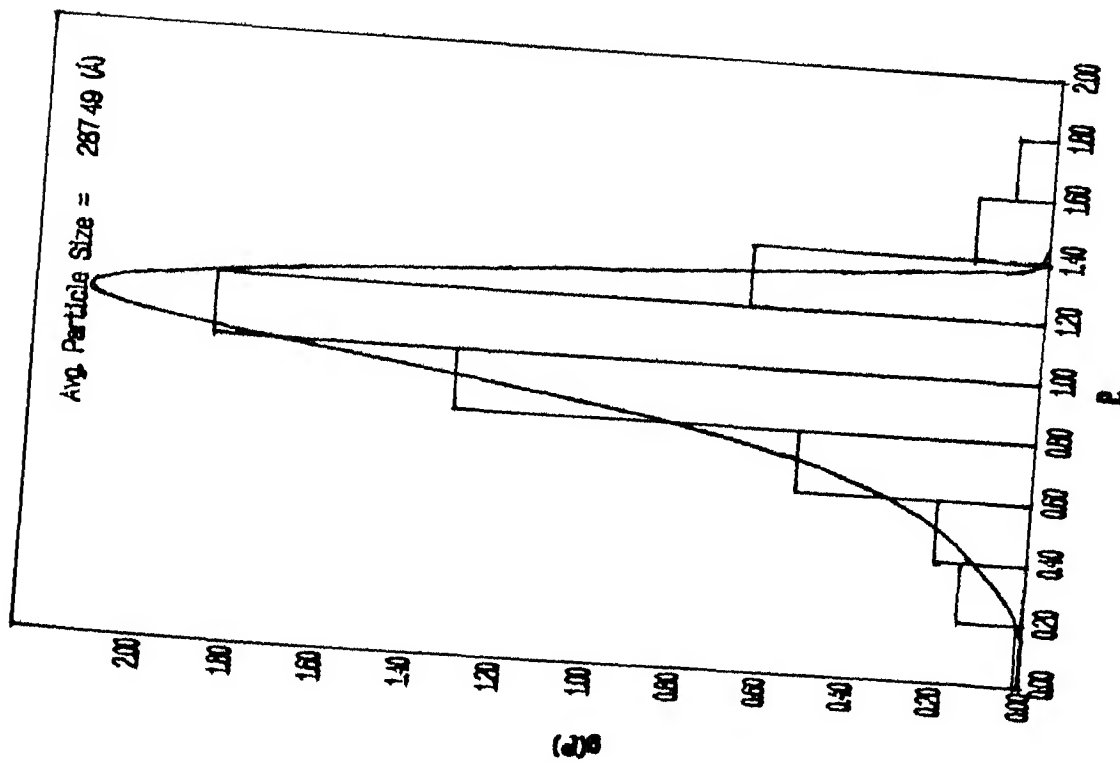
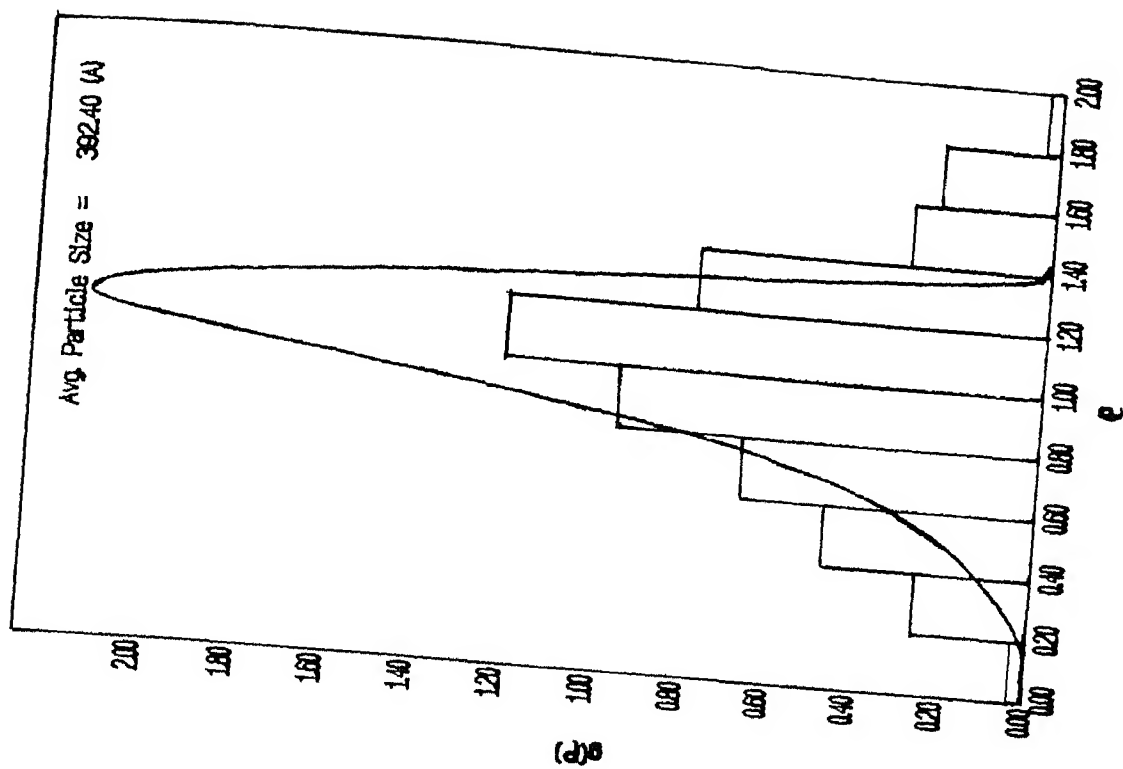


Fig 3 B Particle size distribution, specimen aged at 770°C  
(c) aged for 8 hours (d) aged for 27 hours



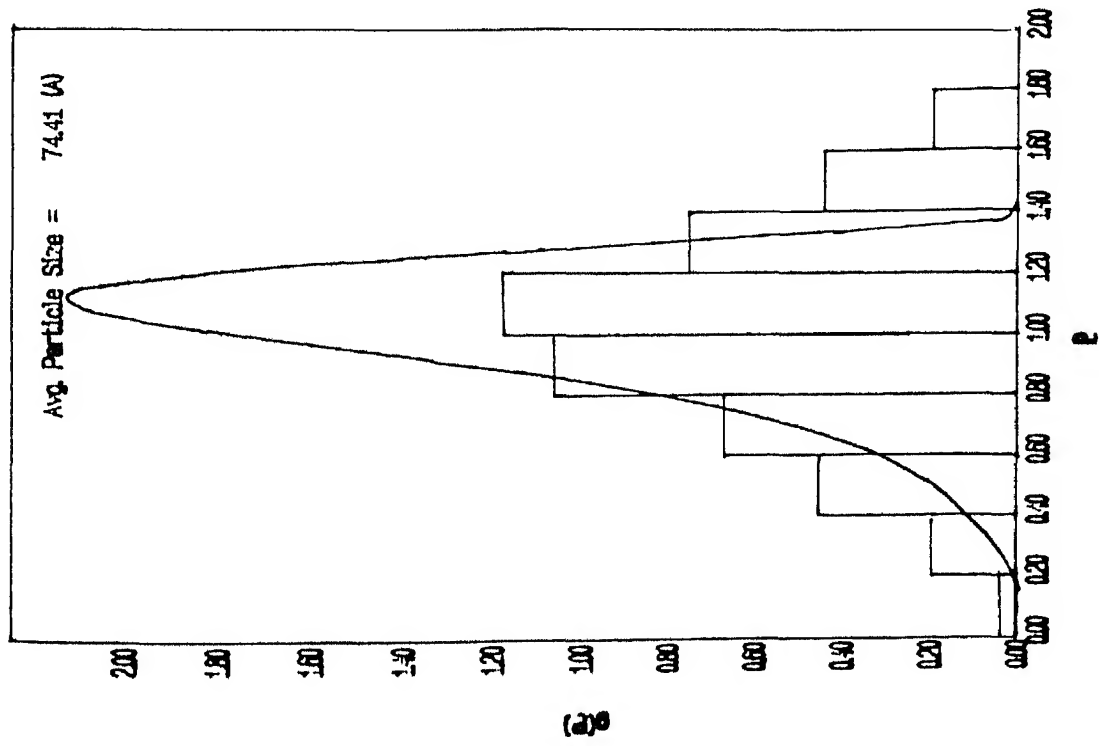
(e)

Fig 3.8 Particle size distribution  
(e) aged for 64 hours

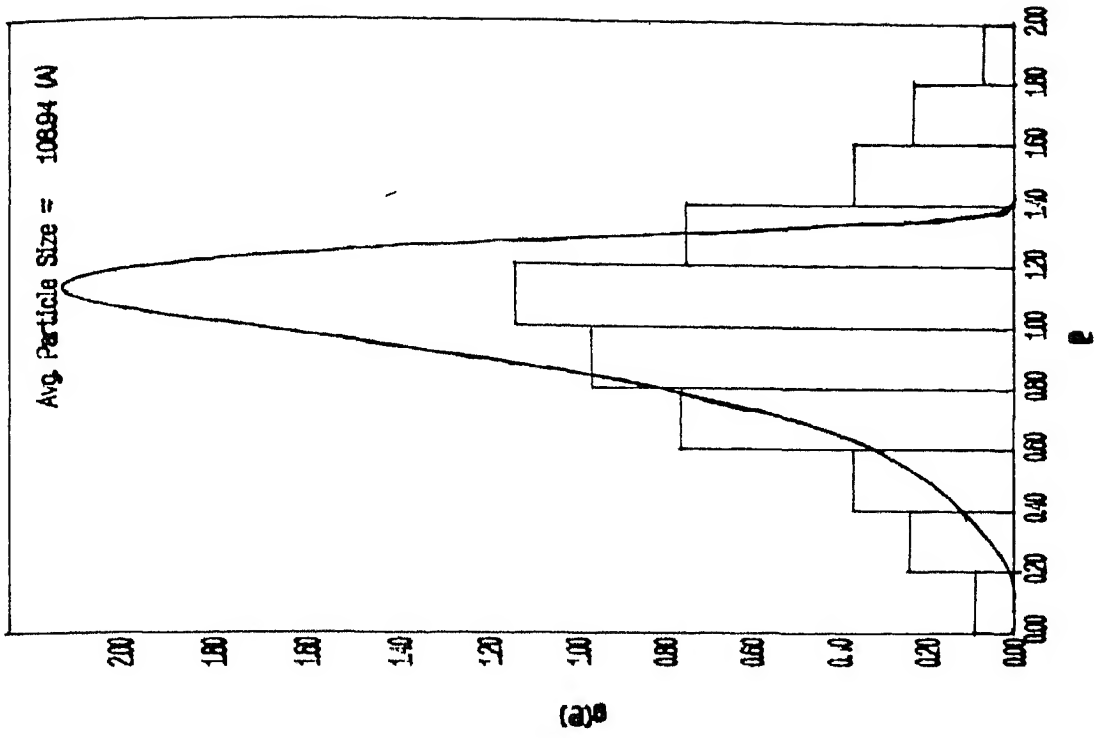


(f)

specimen aged at 770°C  
(f) aged for 216 hours



(a)



(b)

Fig 3.9 Particle size distribution specimen aged at 752°C  
(a) Aged for 8 minutes (b) Aged for 1 hour

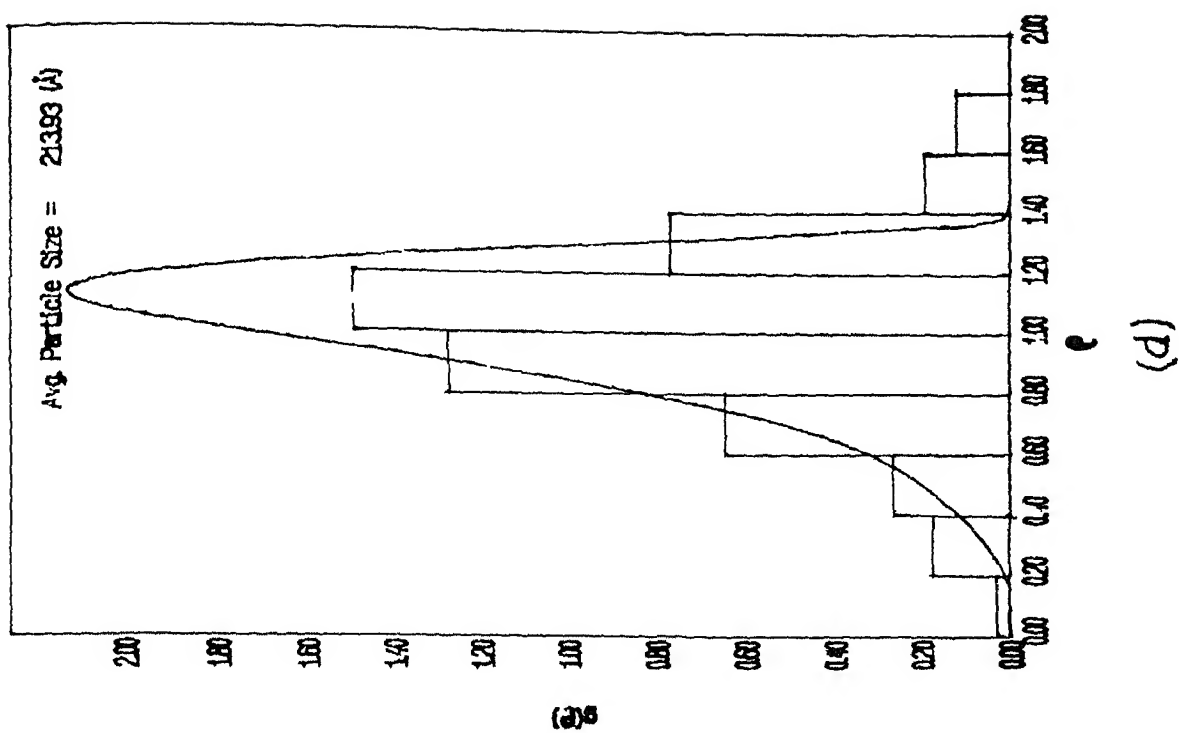
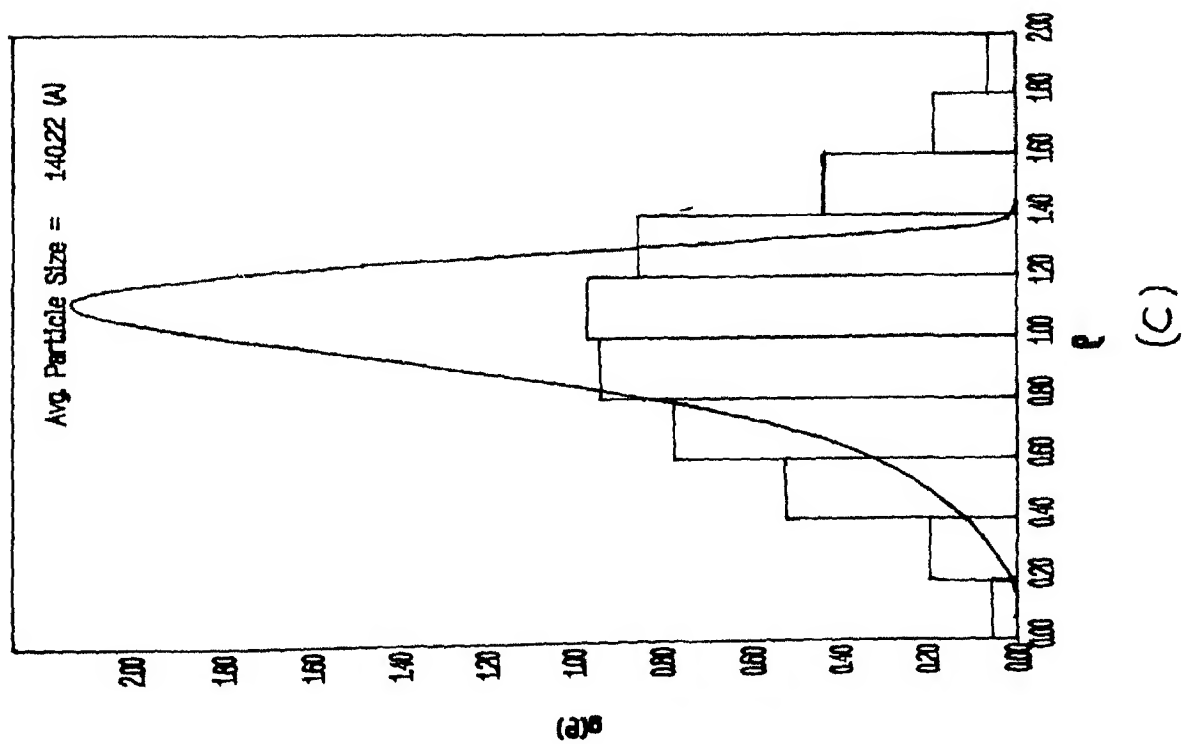
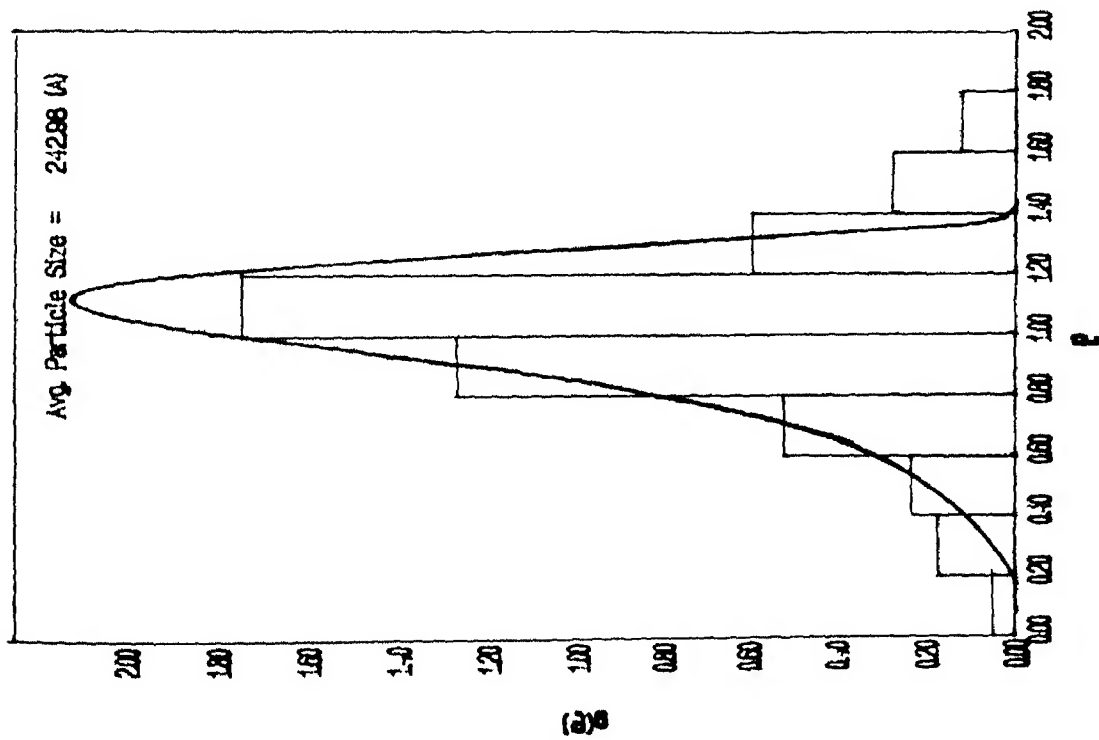
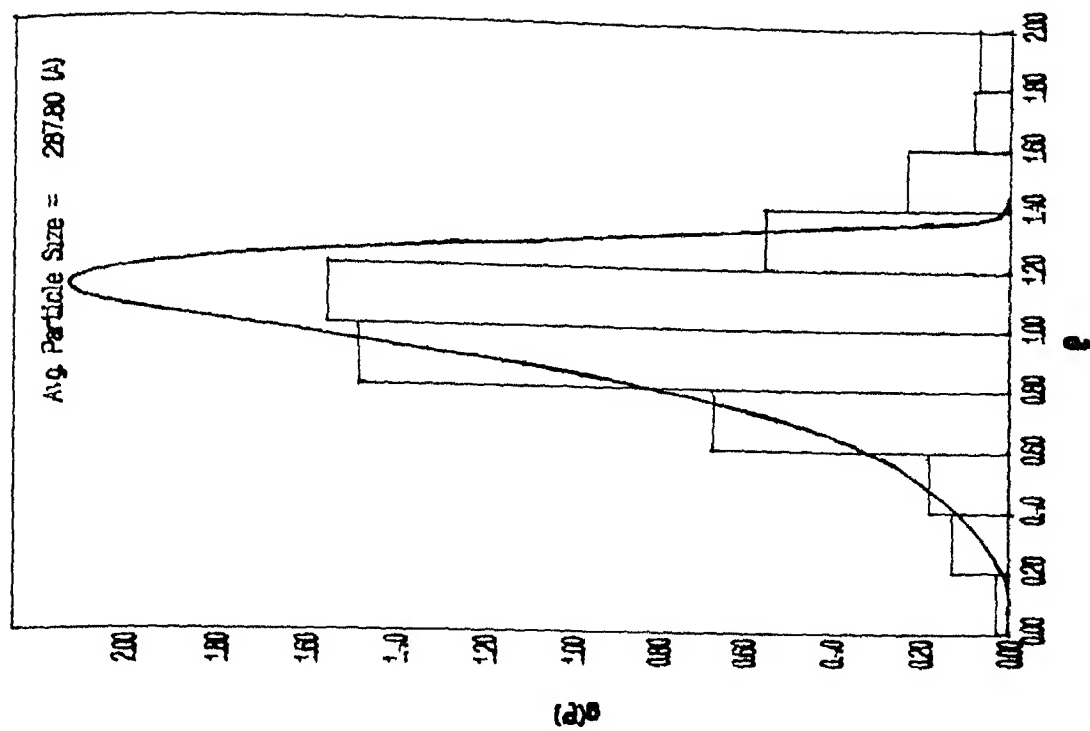


Fig 3.9 Particle size distribution specimen aged at 75°C  
 (c) Aged for 8 hours (d) Aged for 64 hours



(e)



(f)

Fig 3.9 Particle size distribution specimen aged at 752°C  
(e) Aged for 137 hours (f) Aged for 216 hours

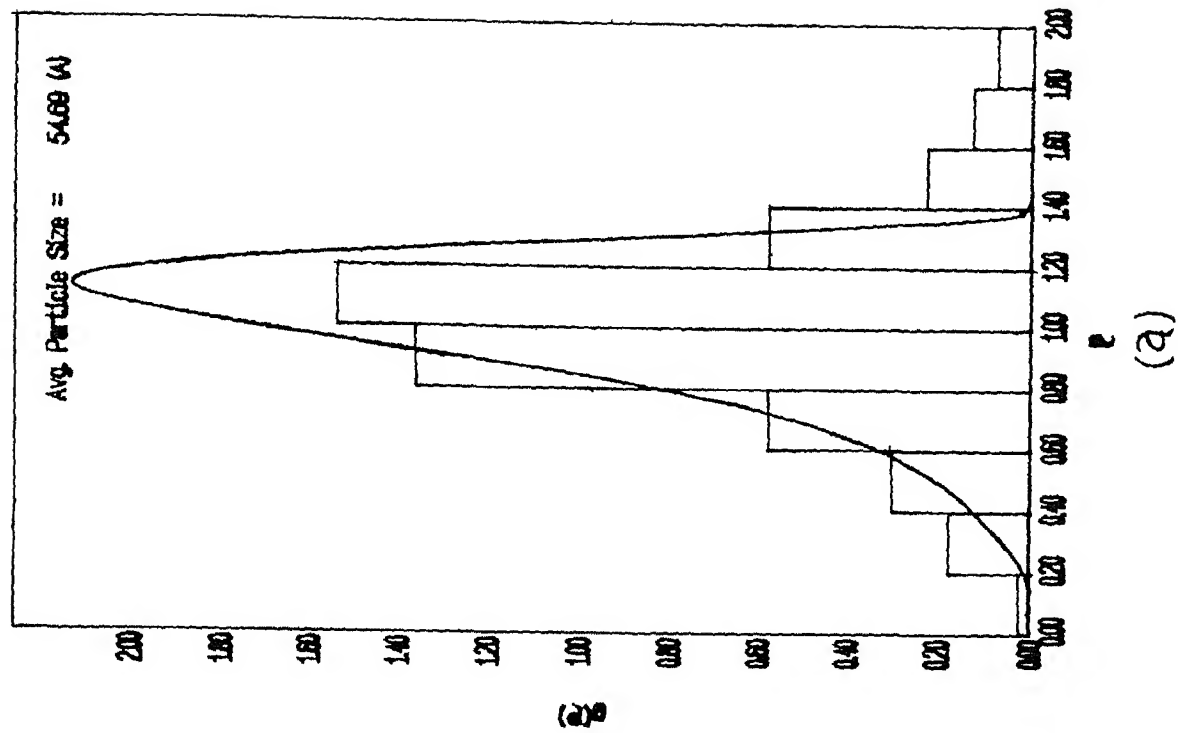
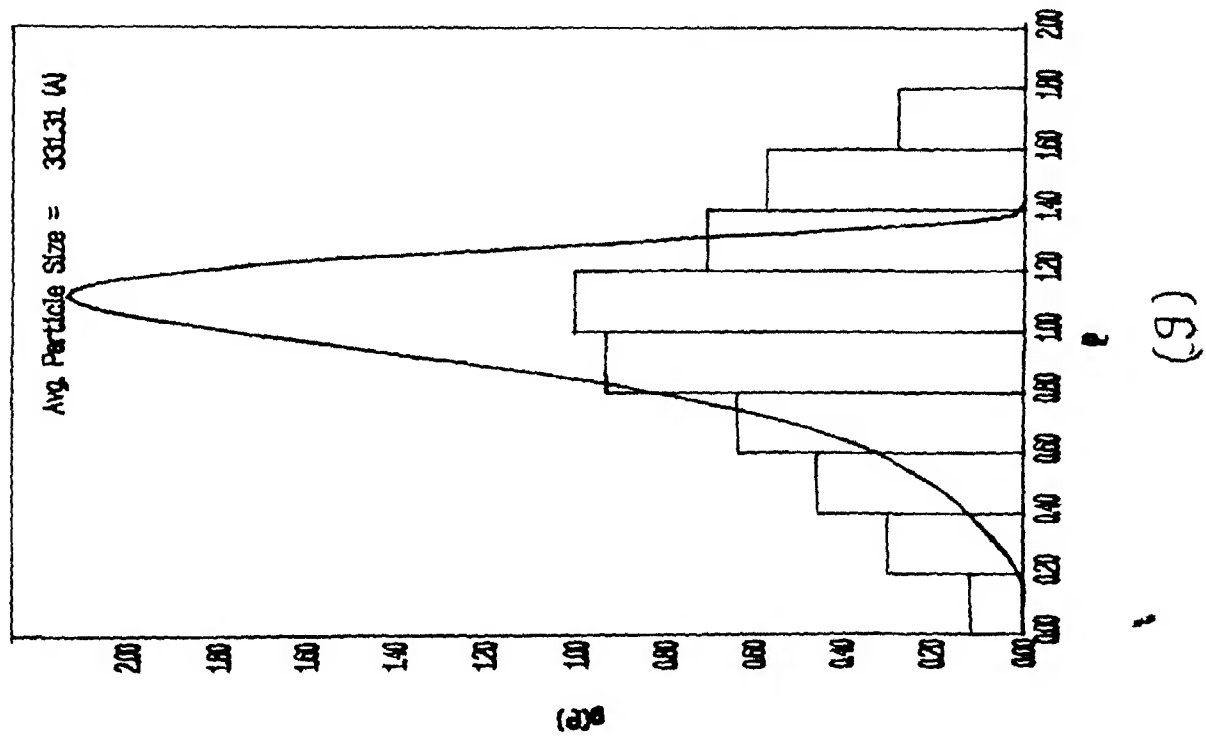
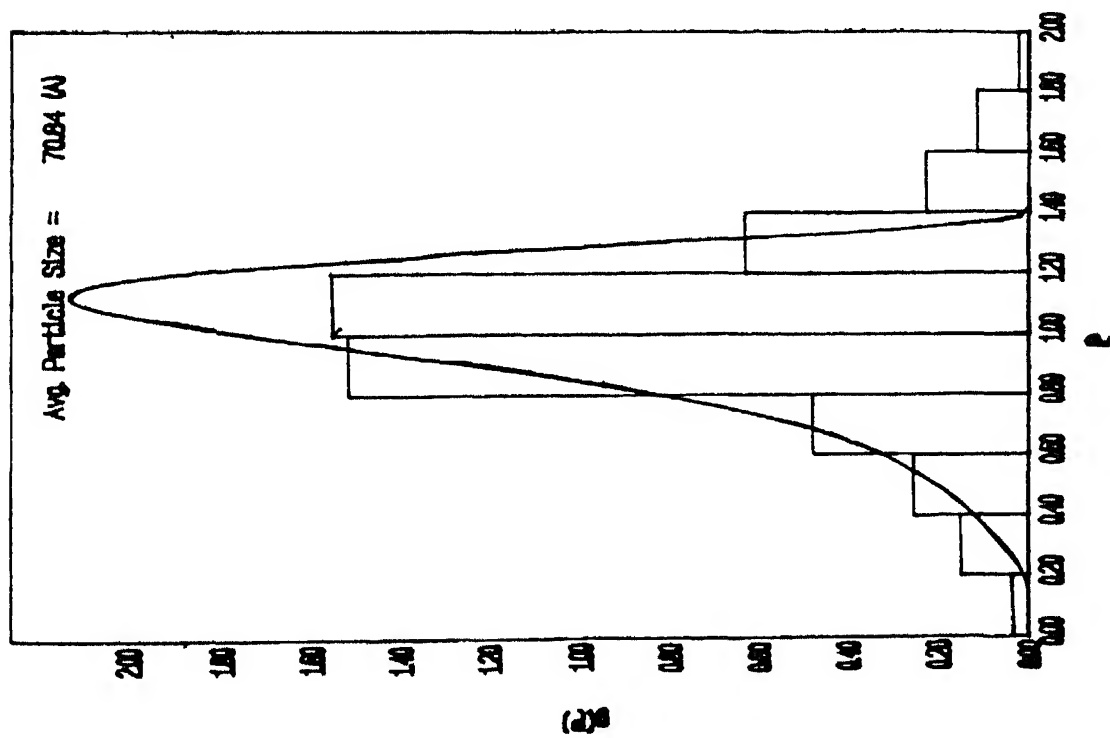
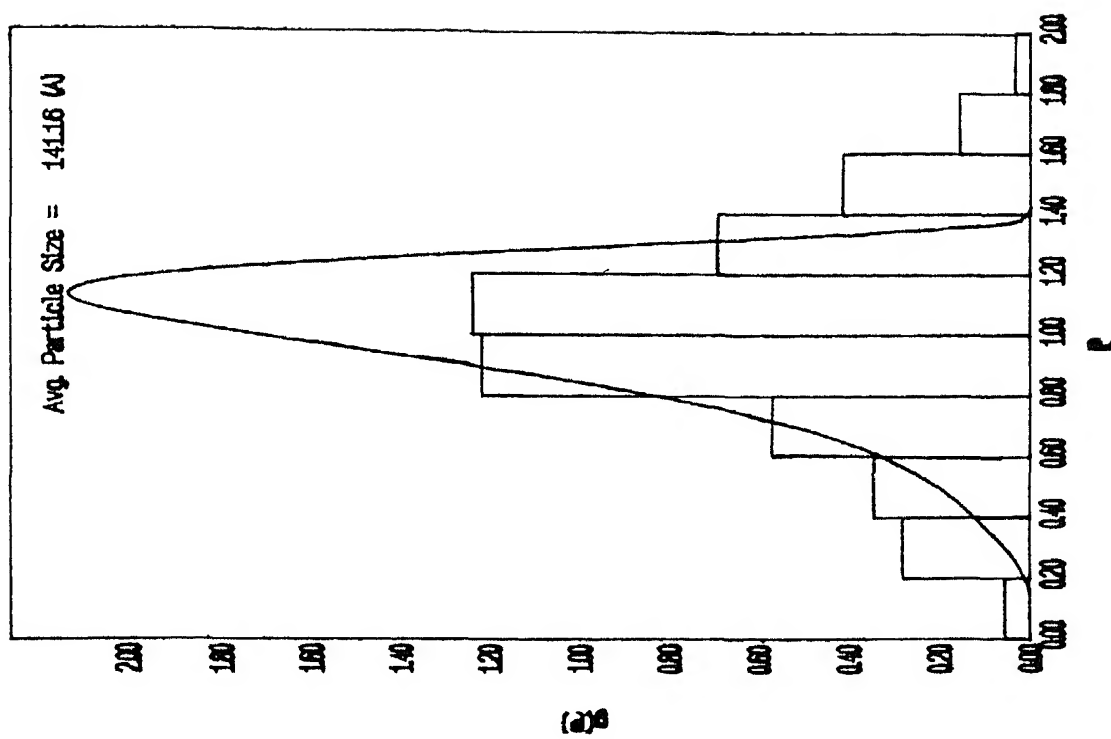


Fig. 3.10 Particle size distribution specimen aged at 752°C (g) Aged for 343 hours (a) aged for 8 minutes





(b)



(c)

Fig 3 10 Particle size distribution specimen aged at 753°C  
 (b) Aged for 1 hour (c) Aged for 64 hours

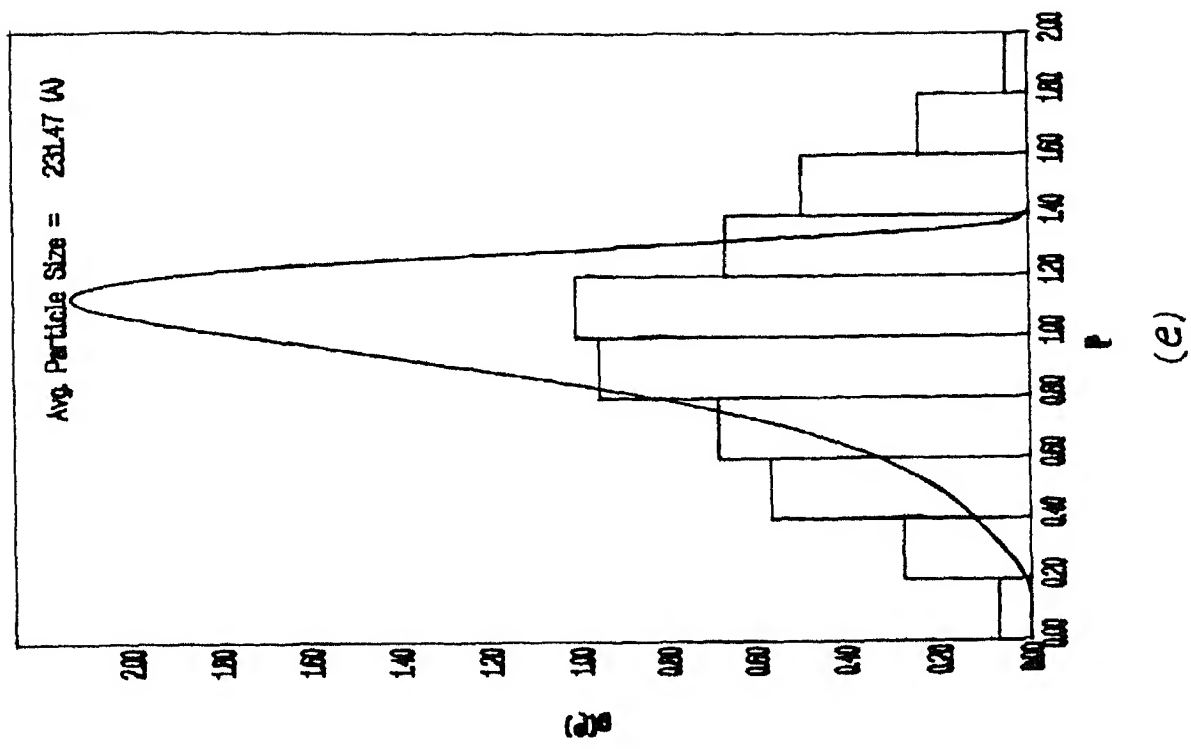
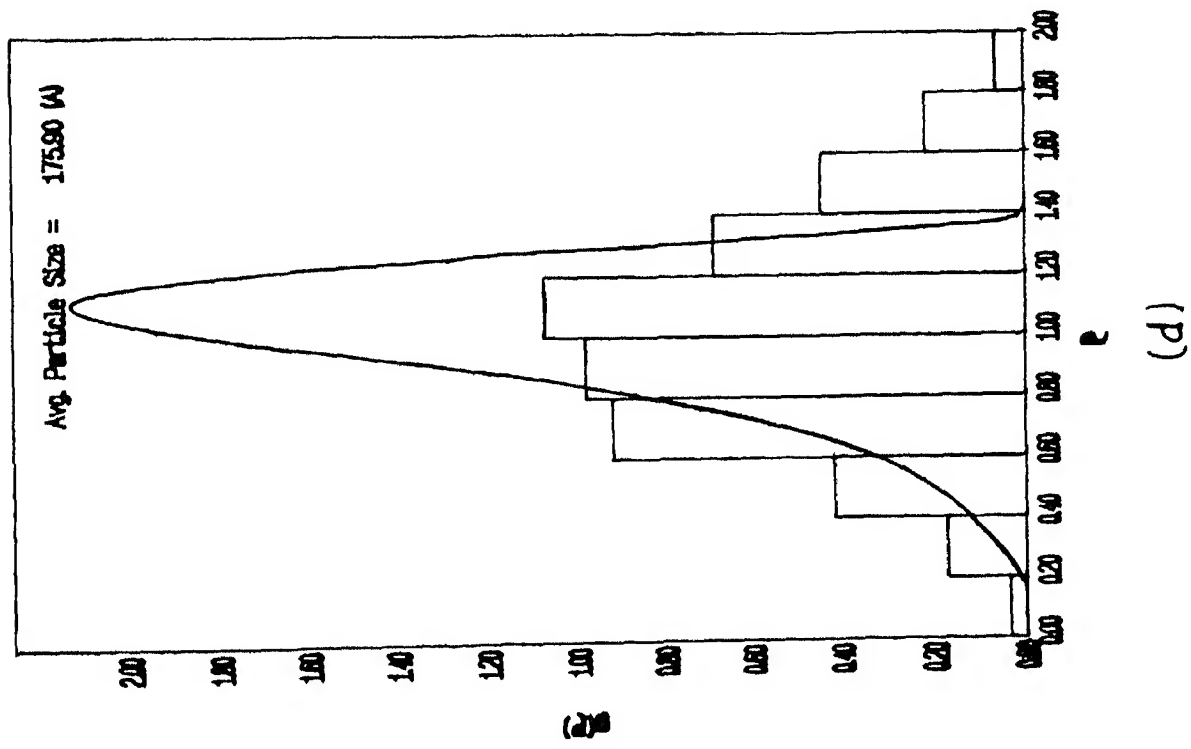


Fig 3 10 Particle size distribution specimen aged at 733°C  
 (d) Aged for 216 hours (e) Aged for 343 hours

1.0-1.4 which is lower than the theoretically predicted value of 2.12 for LSW theory. Exception are observed in few cases where the peak value lies between 1.6 and 1.8.

(d) Instead of being narrow, a number of PSDs were broad near the value as displayed in Figure 3.9(c) and 3.10(d) after coarsening for 8 h at 752°C and 216 h at 733°C respectively.

The above observation for the coarsening of VTiCN are consistent with those reported for vanadium nitride precipitates [14] and vanadium carbide [4]. Recently Mackay et al. [15] have shown that the PSDs during volume diffusion controlled coarsening of the  $\gamma$  phase in Nickel base alloys is a normal rather than a log normal distribution.

In an analysis carried out to study the effect of the volume fraction on the particle size distribution, Ardell [5] has shown that the peak value of  $g(\rho)$  decreases with increasing volume fraction  $\phi$  of the precipitate and the PSD broaden. The broadening is symmetrical about value [Fig. 3.11]. At very large volume fraction of the precipitate, the PSD for volume diffusion controlled coarsening reaches that for interface controlled coarsening. The PSD, however remains asymmetrical as in the LSW [2,3] theory. The Lifshitz-Slyozov encounter modified [LSEM] theory of Davies et al. [7] predicts a normal distribution symmetrical about the mean value and is particularly applicable for alloy system with a small volume fraction of the precipitate [Fig. 3.12]. The basic kinetics equation for the growth remains unchanged.

If the LSEM theory has any validity then one must observe encounter between particles, i.e., coalescence of two or more

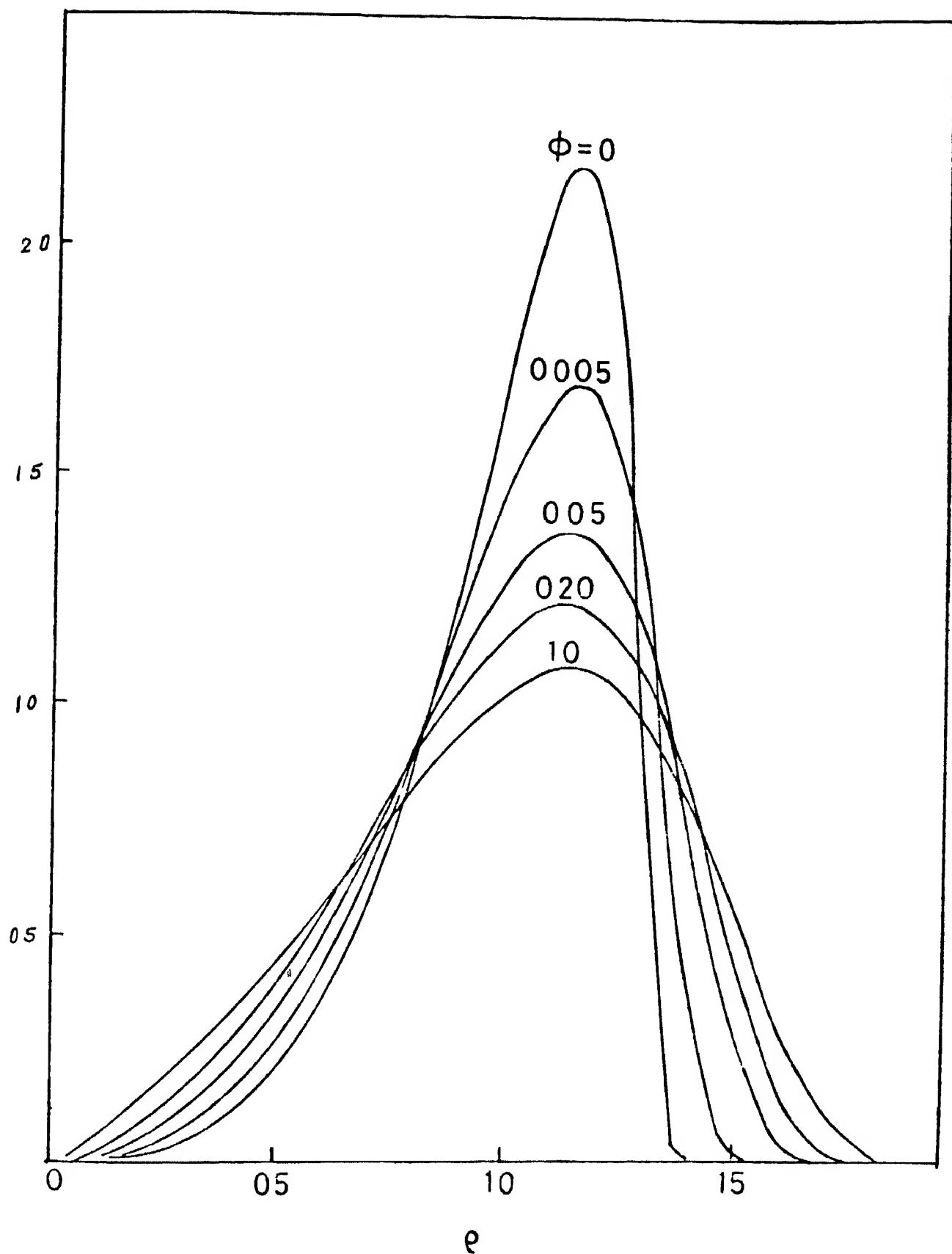


Fig 3 11 Theoretical PSD modified to accommodate the volume fraction of the precipitate [Ref 5]

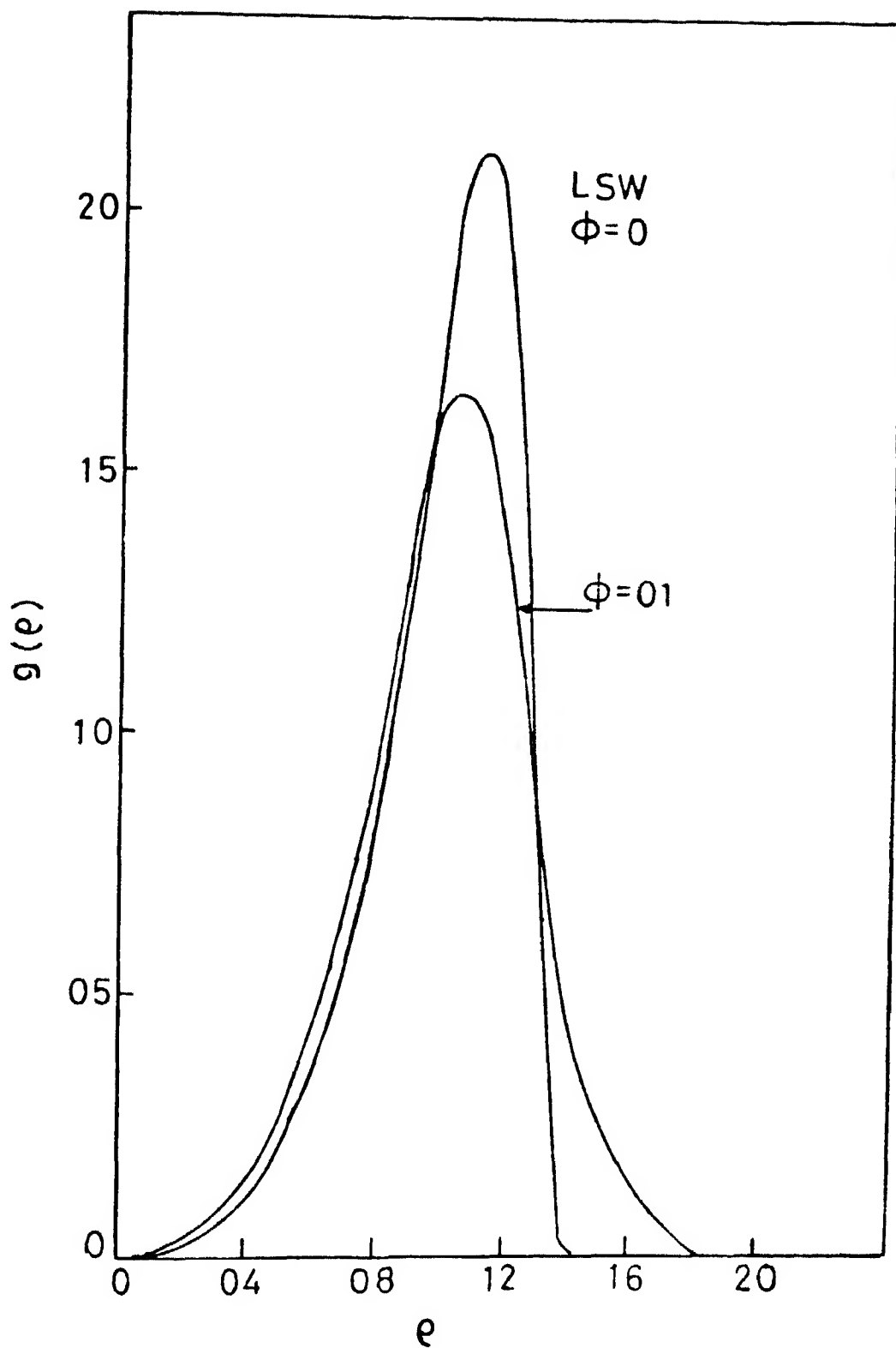


Fig 3 12 Theoretical PSD modified to incorporate the encounters between particles [Ref 7]

neighbouring particles which coarsened by receiving solute from the matrix. During the course of this investigation we observed coalescence between particles in a few specimen. The encounters were between two or more particles in the TEM micrograph of Figure 3.7(b). In some cases the particles were simply lying one above the other. Davies et al. [7] have shown L shaped and a number of rectangular shaped particles of  $\text{Ni}_3\text{Al}$  after 44 hours of aging at  $750^\circ\text{C}$  in a Ni-Co-Al alloy. If the LSEM theory of Davies et al. [7] is applicable it will,

- (i) Modify the PSD so as to be symmetrical about the mean value
- (ii) Increase the cut-off radius ratio to value close to 1.9 or more
- (iii) Broaden the PSD near the mean value, and
- (iv) Lower the peak value of  $g(\rho)$

Although the particle encounter theory of Davies et al. [7] have some merit consistent with the observation both microstructural as well as of particle size distribution, it contributes significantly only when the volume fraction of vanadium Titanium Carbonitride in HSLA Steels containing comparable amount of V, Ti, C and N is reported to be less than 0.01 [16].  $\text{VTiCN}$  does not nucleate homogeneously but nucleates on coherent  $\gamma/\alpha$  interface during ferrite transformation by the ledge mechanism [17,18]. Generally, a large step (ledge height) is followed by several much smaller steps which leads to several closely spaced bands of precipitate followed by a large space to the next band of precipitate [18]. Thus, a large volume fraction of the precipitate is confined within a sheet. In pure Fe-V-C alloys, an inter-plate spacing of the order of 200 to 1000 Å is

reported [19] Because of the large volume fraction of the precipitate, encounters between particles within a sheet and between particles within a row are expected From the shape of the PSDs and micro structural evidence, the encounter modified theory of Davies et al [7] deserves some merit

### 3.3 Kinetics of Coarsening

The kinetics equation describing time dependence of the particle size is derived for spherical or plate shaped particles The Vanadium Titanium Carbonitride (VTiCN) precipitate is cube shaped assumed to have interfacial free energies of the coherent face  $\gamma$  The equation derived by Ramakrishna et al [4] is for plate shaped particle In their equation (1.16)  $\beta = 1$  (length/thickness) is replaced for cube shape particle, the basic equations for volume and interface diffusion controlled coarsening are identical in form to those of the LSW theory For volume diffusion controlled coarsening these are

$$\left(\frac{\bar{a}}{2}\right)^3 = \left(\frac{\bar{a}_0}{2}\right)^3 + \frac{8}{9} \frac{D_v \gamma \sqrt[3]{\omega_B^\beta} \omega_B^\alpha}{\alpha RT (X_B^\beta X_B^\alpha)} t \quad (1.20)$$

Taking the approximate form of the above equation, the average value of the particle size,  $\bar{a}$  ( $\text{\AA}$ ) is plotted against cube root of the time  $(t)^{1/3}$  at the three temperatures used in this study Figure 3.13 clearly shows that the average particle size data fits the  $t^{1/3}$  proportionality The experimental data for volume diffusion controlled growth are shown in Table 3.1

The coarsening kinetics therefore appears to be volume diffusion controlled as also reported for Fe-Mo-C [20], Fe-Ti-Si [21] and Fe-V-C [4] alloys The data of Figure 3.13 were fitted

Table 3 1

Average Particle Size with respect to Time and Temperature

Temperature (°C)	Aging Time (h)	Average Particle Size Å
770	1	139 62
770	8	212 02
770	27	254 25
770	64	287 49
770	216	392 40
752	1	108 94
752	8	140 22
752	64	213 93
752	137	242 98
752	216	287 80
752	343	331 31
733	1	70 84
733	64	141 16
733	216	175 90
733	343	231 47



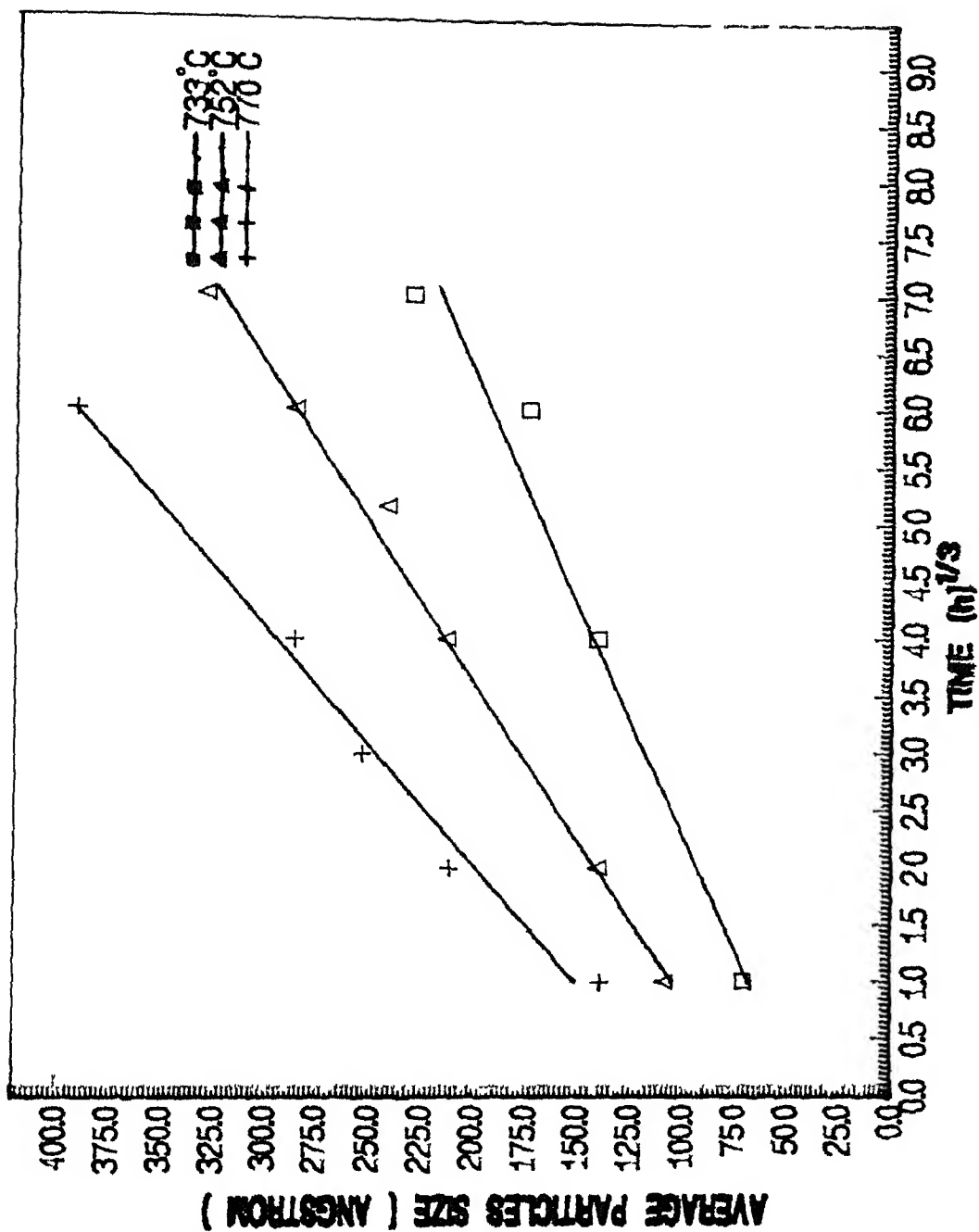


Fig 3 13  $\bar{a}$  versus  $t^{1/3}$  plot for the coarsening of vanadium Titanium Carbonitride (VTiCN) in HSLA Steel

to linear least square constant ( $\bar{a}_0$ ) and slope  $K^{1/3}$ , thus determined are shown in Table 3 2

In an attempt to get some idea of the atomic specie controlling the rate of coarsening, the equation (1 18) was used and calculation of the diffusion coefficient  $D_v$  made at the three temperatures. The constant  $\gamma$  in this equation is dependent upon the interfacial energy of the edge with the  $\alpha$  matrix, the parameter  $\alpha$  and  $\beta$ , mole fraction of solute in the  $\alpha$  phase in equilibrium with a very large size precipitate,  $^{\infty}X_B^{\alpha}$ , the molar volume of the vanadium-titanium carbonitride (VTiCN) and the difference  $(X_B^{\beta} - X_B^{\alpha})$

From the crystal structure (FCC) and the published lattice parameters which falls in the range 4 138 to 4 182Å for  $VC_{0.75}$  to  $VC_{0.961}$  and in the range 4 3127-4 328Å for  $TiC_{0.61}$  -  $TiC_{1.0}$ . Taking the approximate value of the lattice parameter to be 4 25Å for TiVCN. It gives the value of  $V_M^{\beta}$  to be  $11.558 \times 10^{-6} m^3/mole$ . For  $^{\infty}X_B^{\alpha}$ , we used B= carbon and determined the mole fraction of carbon in ferrite at various temperatures from the equilibrium Fe-C phase diagram. This is approximate only. The exact value can be obtained from the  $\alpha/(\alpha+VTiC)$  boundary in a steel containing 0 185V, 1 50 Mn. Since  $X_B^{\alpha}$  is very small compared to  $X_B^{\beta}$  the difference  $(X_B^{\beta} - X_B^{\alpha})$  is taken to be  $\approx 0.45$  for VTiCN. The parameter  $\alpha$  is treated as a constant with a value equal to unity.  $\alpha$  is not a constant but is dependent upon the particle size as shown by Shiflet et al [22].

The interfacial free energy as the coherent broad face is expected to be low and comparable to the coherent twin boundary energy of  $30 mJ/m^2$  [23]. On this basis alone the interfacial

Table 3 2

Value of the Constant ( $\bar{a}_0$ ) and Slope ( $\gamma^{1/3}$ )

Temperature °C	$\bar{a}_0$ (Å)	$\gamma^{1/3}$ (Å/h <sup>1/3</sup> )	$\gamma$ (m <sup>3</sup> s <sup>-1</sup> )
770	78 22	46 26	27 5 × 10 <sup>-30</sup>
752	74 41	36 67	13 78 × 10 <sup>-30</sup>
733	54 69	23 48	3 6 × 10 <sup>-30</sup>

Table 3 3

Values of  $K$ ,  $\alpha_X^\alpha$ ,  $D_V$  experimental and Calculated

Temperature	770°C	752°C	733°C
$K, m^{-3} s^{-1}$	$27.5 \times 10^{-30}$	$13.78 \times 10^{-30}$	$3.6 \times 10^{-30}$
$\alpha_X^\alpha$	$1.486 \times 10^{-3}$	$1.72 \times 10^{-3}$	$2.135 \times 10^{-3}$
$D_V$ , Experimental $m^2 s^{-1}$	$1.952 \times 10^{-18}$	$0.830 \times 10^{-18}$	$0.171 \times 10^{-18}$
$D_V, m^2 s^{-1}$ Ramakrishana et al [4]	$0.16 \times 10^{-18}$	* $0.09 \times 10^{-18}$	** $0.05 \times 10^{-18}$
$D_V, m^2 s^{-1}$ Bowen et al [25]	$282 \times 10^{-18}$	* $168 \times 10^{-18}$	** $92 \times 10^{-18}$
$D_V, m^2 s^{-1}$ Bowen et al [26]	$2.7 \times 10^{-18}$	* $1.4 \times 10^{-18}$	** $0.8 \times 10^{-18}$
$D_V, m^2 s^{-1}$ Mall et al [27]	$111 \times 10^{-18}$	$67 \times 10^{-18}$	$12 \times 10^{-18}$

\* at 750°C

\*\* at 730°C

energy of the edge can be computed to be about  $110 \text{ mJ/m}^2$ . The average energy of the edge can be taken as approximately  $250 \text{ mJ/m}^2$  which is lower than the grain boundary energy ( $700 \text{ mJ/m}^2$ ) of ferrite and interfacial energy of  $700 \text{ mJ/m}^2$  for the Fe/Fe<sub>3</sub>C interface [24] at  $710^\circ\text{C}$ .

The value of  $D_v$  was calculated from approximate values of the parameters in equation (1.18) as shown in Table 3.3. The diffusivity values of this investigation are comparable to the  $D_v$  values obtained by Ramakrishna et al. (V in  $\alpha$ -Iron) [4], which is very much close to value obtained by Bowen et al. (V in  $\alpha$ -Iron) [25] and the experimental  $D_v$  values differ from those obtained by Bowen et al. (V in  $\alpha$ -Iron) [26] and Moll et al. (Ti in  $\alpha$ -Iron) [27] by an order of magnitude two. The data compare very favourably with the experimentally observed  $D_v$  values. From these  $D_v$  values at different temperature, activation energy ( $Q$ ) and  $D_0$  can be calculated. However, due to insufficient points the calculations of  $Q_v$  and  $D_0$  were not made.

## CHAPTER 4

### CONCLUSIONS

The rate of growth of Titanium Vanadium Carbonitride in HSLA Steel exhibited cube rate law behaviour and volume diffusion controlled mechanism predicted by the LSW theory of particle coarsening. The LSW theory as well as several modified theories were ineffective in describing the experimentally determined particle size distribution. The experimentally observed PSDs follow a normal distribution rather than a log-normal distribution. There is some evidence of the modification of the PSDs by encounters between particles. However, the exact contribution that they make in modifying the PSDs is not known. The experimental particle size distribution differ with respect to the peak value, cut off radius ratio and shape of predicted PSDs from theoretical considerations. Using estimated value of the parameter of the kinetics equation, the experimental diffusivity,  $D_v$ , values are comparable with the calculated  $D_v$  values as they lie within an order of magnitude of each other.

## REFERENCES

- 1 W Ostwald, Z Phys Chem (Leipzig), 34 (1900), p 495
- 2 I M Lifshitz and V V Slyozov, J Phys Chem Solids, 19 (1961), p 35
- 3 C Wagner, Z Electrochem, 65 (1961), p 61
- 4 D Ramakrishna and S P Gupta, 92 (1987), p 179 *Mat Sc Engg*
- 5 A J Ardell, Acta Metallurgica, 20 (1972), p 61
- 6 G W Greenwood, Acta Metallurgica, 4 (1956), p 243
- 7 C K L Davies, P Nash and R N Stevens, Acta Metallurgica, 28 (1980), p 179
- 8 A D Brailsford and P Wynblatt Acta Metallurgica, 27 (1979), p 489
- 9 C S Jayanth and P Nash, J Mater Sci , 24 (1989), p 3041
- 10 P W Voorhees and M E Glicksman, Acta Metallurgica, 32 (1984), p 2013
- 11 P J Goodhew, Specimen preparation in Material Science, Newyork, (1973)
- 12 J M Gray and R B G Yeo, Trans ASM, 61 (1968), p 255
- 13 P Merle and F Fouquet, Acta Metallurgica, 29 (1981), p 1919
- 14 O E Atasoy, Metall Trans A, 14 (1983), p 379
- 15 R A Mackay and M V Nathal, Acta Metallurgica, vol 38, 6 (1990), p 993
- 16 A D Batte and R W K Honeycombe, Met Sci , J , 7 (1973), p 160
- 17 K R Kinsman and H I Aaronson, Met Trans , 4 (1973), p 959

- 18 R W K Honeycombe, Metall Trans A , (1976), p 915
- 19 N K Balliger and R W Y Honeycomb, Met Trans A , 11A  
(1980), p 421
- 20 D M Davies and B Ralph, J, J Iron Steel Inst , London, 210  
(1972), p 262
- 21 E Bower and J A Whitemann, The Mechanism of Phase  
Transformation in Crystalline Solids, Institute of Metals,  
London, (1968), p 119
- 22 C J Shiflet and H I Aaronson, Acta Metallurgica, 27 (1979),  
p 377
- 23 M Mclean and H Mykura, Acta Metallurgica, 12 (1964), p  
326
- 24 J J Kramer, G M Pound and R F Mehl, Acta Metallurgica, 6  
(1958), p 763
- 25 A W Bowen and G M Leak, Metall Trans , 1 (1970), p 2767
- 26 A W Bowen and G M Leak, Metall Trans 6 (1970), p 1965
- 27 S H Moll and R E Ogilvie, Trans Metall Soc , AIME, 215  
(1959), p 673



## APPENDIX

### COMPUTER PROGRAM FOR PARTICLE SIZE DISTRIBUTION

```
#include <stdio.h>
#include <string.h>
#include <math.h>
char sample_name[100];
float real_size[100][100]; overall_avg_size avg_size
int number_of_particle [ 0] no_magnifications
int particle_density[ 0]

main()
{
    float size[ 0][ 0];
    float magnitude_of_magnif[20];
    char file_name[100] plot_file[10] dec[5];
    int part_no[ 0] n_color;
    FILE *fp; fopen() *tempf;
    int i j k number_of_particles rem_par;
    float dummy_size[ 0][0] dummy[5000];
    float magn_den;
    float low_bound upper_bound range;
    float min_size n_x_size;
    int tot_par;
    tot_par = 0;
    while (1)
    {
        printf( "GIVE THE FILE NAME CONTAINING sample_name number of particles & sizes\n" );
        scanf( "%s %d %d", &file_name, &no_magnifications, &n_color );
    }

    /* **** READ DATA FROM THE GIVEN DATAFILE ***** */

    if (fp = fopen(file_name, "r"))
    {
        fprintf(fp, "sample_name\n");
        fprintf(fp, "%d no_magnifications\n", no_magnifications);
        for (i = 0; i < no_magnifications; i++)
        {
            fprintf(fp, "%d part_no[i]\n", part_no[i]);
            fprintf(fp, "%d magnitude_of_magnif[i]\n", magnitude_of_magnif[i]);
            fprintf(fp, "%d number_of_particles[i]\n", number_of_particles[i]);
            for (j = 0; j < number_of_particles[i]; j++)
            {
                fscanf(fp, "%f", &real_size[i][j]);
            }
        }
    }

    /* **** CALCULATE THE REAL SIZE OF THE PARTICLES ***** */

    real_size[i][j] = real_size[i][j] * 1.0e+07 / magnitude_of_magnif[i];
    dummy_size[i][j] = real_size[i][j];
    ++i;
}

/* **** MINIMUM SIZE MAXIMUM SIZE OVERALL AVERAGE PARTICLE SIZE CALCULATION **** */

min_size = (real_size[0][0] > real_size[0][1]) ? real_size[0][1] : real_size[0][0];
max_size = (real_size[0][0] > real_size[0][1]) ? real_size[0][0] : real_size[0][1];
for (i = 0; i < no_magnification; i++)
{
    for (j = 0; j < number_of_particles[i]; j++)
    {
        if (real_size[i][j] < min_size) min_size = real_size[i][j];
        if (real_size[i][j] > max_size) max_size = real_size[i][j];
    }
    tot_par++;
}

overall_avg_size = sum(dummy_size) / tot_par;

printf( "min_size = %f\n", min_size );
}
```

```

INITIALIZATION
      *          */
      /
      g       o erall_a g_ size
rem_par tot_par
low_bond    0 0
upper_bond  0   o e all_avg_size
n           0

DIVID TH PARTICLE SIZE AXI INTO 10 EQUAL DIVISIONS
CALCULATION OCCUR UNTIL NO PARTICLE FALLS BEYOND TWICE
THE AVERAGE PARTICLES SIZE

while (n < rem_par)
{
max_dens = 0 0
}
particle_density[i] = 0
while (upper_bond < 0+avg_size)
{
for (j = 0 ; j < rem_par + 1 ; j++)
if ((dummy_size[j] > lower_bond) && (dummy_size[j] < upper_bond))
{
dummy_size[j] = dummy_size[j]
particle_density[j]++
}
}
max_dens = (max_dens > particle_density[k]) ? max_dens : particle_density[k]
lower_bond = upper_bond
k
upper_bond = 0 + avg_size
particle_density[k] = 0
}
avg_size = 0 0
for (i = 0 ; i < m ; i++)
{
avg_size += dummy_size[i]/m
dummy_size[i] = dummy_size[i]
}
lower_bond = 0 0
upper_bond = 0 + avg_size
if (m == rem_par)
{
rem_par = n
n = 0
}
}
number_of_packets = k + 1
tot_particles = rem_par

create dist(0 0 0 0 0 (<= 0 max_dens)/tot_particles 0 2 10 particle_density tot_particles)
output distribution(number_of_packets tot_particles particle_density)

HISTOGRAM ***** */
print("DO YOU WANT TO HOW THE SIZE DISTRIBUTION ON HISTOGRAM(y/n) ")
do {
getchar()
if (do {
getchar()
y } )
{
x = rem_particles
printf("GIVE THE NUMBER OF COLORS (1 to x) ? ")
scanf("%d",&dci)
if (dci != 0) printf("WANT TO OVERLAP THE IDEAL CURVE (yes/no) ? ")
scanf("%c",&dci)
x = ideal_particles(dci)
x = color_files(x,dci,color)
}
```

```

printf( "\nWAIT " )
sy t l / 1/r g/hg aph </s21/mkag/inp_histo >/s21/mkag/file out )
) irtf( PL)ITTER FILE (y/n) ? )
q tcha ()
if (qe c () y )
(
q tch ()
if( IVE THE PLOTTER FILE NAME )
ec rt( [ r] plct_file)
ftp foper( d p w )
fr irtf(ffr r plot_file)
f ri lf(ff 17 n )
fc l e(f )
y tem( cat dur >>inp_pl tter )
ystem( s 1/m g/histo/hg aph </s21/mkag/inp_plotter >/s21/mkag/file out )
system( rm fle ut dup )
)
)

/
END OF THE MAIN PROGRAM
****

ROUTINE TO MAKE DATAFILE FOR HISTOGRAM ***** */

c t d i (xmr xmax ymin ymax interval no_points particle_no tot_no_par)
t)( t xmr xm ymin /m x interval)
int ic pcints particle_no[20] tot_no_par
(
IL idfp if p n()
int i
dfr foper( IZE_DI TRIBUT w )
tprintf(drp 1\ r )
tprintf(drp 1\ i )
rp irtf(drp f\t/f\t r\t\tf\n xmr xmax ymin ymax)
rprir t(drp i r )
fp irtf(drp 1\ r no_poi ts)
for (i 1 i no_points i++)
ffri tf(drf /f r ( 0+particle_no[i])/tot_no_par)
fclos (drp)
)

/*
ROUTINE FOR NUMERICAL OUTPUT (STD OUT/TO FILE) *****/

output_detail(point tot_no_par particle_density)
rt p irt tot_ro_par p rticle_density[20]

extern r sample_name[18]
extern flc t real_1 e[20][ 00] overall_avg_size avg_size
fl t a y_ro_par[ 0]
fl at lower bond upper_bond
irt i i k n
(char decision outfile[ 0])
FILE * ) *fio n()
q ch i()
) /f( OUTPUT IS REDIRECTED TO ONE FILE(y/n) )
ca f( / &de ion)
if ( e i irr i y )
(
fr i tf( s n sample_ ame)
p irtf( A TICLE IZ ( Anq trom)\n\n )
f i tf( _____ \n\n )
(
k i
for (i 0 i no_ragrifications i++)

```

[illegible]

```

tprn tf(1fp / f\ )
fprintt(1fp / r\ )
fprintt(1fp n )
fprintt(1fp 0 \ )
fp 1 tf(1fp 0 \r )
tf tf(1fp (\r )
tprintt(1fp \ )
tprintt(1fp u 0
fprintt(1fp u u\ )
fp 1 t(1fp 0 u\ )
tprn tf(1fp \r )
fp 1 tr( fp 10\r )
fprintt(1fp \n )
fprintt(1fp o( )\n )
tprintt(1fp A<TICL IZE DI TRIBUTION\n )
fprintt(1fp (\r )
fprintt(1fp \r )
fprintt(1fp 0 3\n )
tprn tf(1fp 4 r )
tprintt( fp 1 r )
fp tf(1fp (\n )
fp trtf( fp 0 7 u n )
tprintt(1fp A o a ticle ize /s (A)\n size)
fprintt(1fp 7\ )
fprintt(1fp 13\ )
tprintt(1fp hp9 0\r )
tprintt(1fp 17\ )
fclose(1fp)
ffp foper( inf_plotte w )
fprintt(1fp IZE_DISTRIBUT\n )
tprintt(1fp 3\ 0 7\n 0 4\n )
fprintt(1fp \r )
for (i 0 ( ro_bars 1 1++)
f 1 tf(1fp 3\n\ 1 r)
f r1 tf( f1 4 )
f r1 tf(1fp / 1\1\n color colo )
f r1tf(1fp 1\ )
f r1tf(1fp y r )
f1 r1tf(1fp \ )
f r1tf(1fp // f\n )
f r1tf(1fp 2f\n )
f r1tf(1fp \n )
f r1tf(1fp 0 n )
f r1tf(1fp 0 \n )
f1 r1tf(1fp 1 )
f r1tf(1fp 3 r )
f1 r1tf(1fp 0 0 n )
f r1tf(1fp 0 0 )
f r1tf(1fp 0 01 )
f r1tf(1fp \n )
f1 r1tf(1fp 10 n )
f r1tf(1fp P\n )
f1 r1tf(1fp q(P)\n )
1 r1tf(1fp PARTICLE IZE DISTRIBUTION\ )
1 r1tf(1fp 7 n )
f r1tf(1fp \r )
t r1tf(1fp 0 3\n )
f r1tf(1fp 4 r )
f r1tf(1fp 1 n )
1 r1tf(1fp h )
f 1 tf(1fp ( 7 \n )
1 r1tf(1fp A q Pa t cle iz /s (A)\n size)
f r1tf(1fp 7\r )
f r1tf(1fp 14 )
cl f

```

```

m te_10r l cu c(dec1)
char dec l ]

```

```

(
FILE if1 *f n()
f1 + y
if( fopen( / i ntag/h1 to/IDEAL_CURVE w )
f r i ( f \ d i)
f r i f( f i 7\n )
t ( 0 0 (- 1 371 x + 0 01)
+ (( 1 ) & ((x < 0 03999) || (x > 0 14011)))
{
( 0 1 87 0 610103*x 3 0245 x*x 1 46649*exp(3 0 log(x))-5 36198 exp(4 0*log(x))
/ 7 3 071 exp( 0*log(x)) 0 5 3 4 exp(6 0 log(x))+0 802699*exp(7 0 log(x))-2 27141 exp(8 0*log(x))
fpr tf1itp + t/f\n x y)
}
el if ((x > 1 ) && (x < 1 37))
{
74 ( 3 6727*x-5 619 x x+12 6906*exp(3 0 loc(x))-13 7876*exp(4 0 loc(x))
/ 47 47 exp( 0 log(x)) 1 0183 exp(6 0*log(x))+0 087391 exp(7 0*log(x)) 9 86829*exp(8 0 log(x))
407 exp(9 0*log(x))
fpr1 tf1itp /f t/r\n x y)

fprintf(1fp 1 314\%0 017 \n )
fprintf( 1fp 1 4\%0 01 \n )
fprintf(1itp 1 417\%0 00 \n )
fprintf(1itf 1 434\%0 0000\n )
fclose(1fp)
}

```

---



---



---